Ground Improvement in Transport Geotechnics - from Theory to Practice

Prof. Buddhima Indraratna
Professor of Civil Engineering & Research Director
Centre for Geomechanics and Railway Engineering
Program Leader, ARC Centre of Excellence in Geotechnical Science & Engineering
University of Wollongong, NSW 2522 Australia

Dr. Sanjay Nimbalkar
Research Fellow, Centre for Geomechanics and Railway engineering
University of Wollongong, NSW 2522 Australia

A/Prof. Cholachat Rujikiatkamjorn
Associate Professor, School of Civil, Mining & Environmental Engineering
University of Wollongong, NSW 2522 Australia

Dr. Ana Heitor
Lecturer, School of Civil, Mining & Environmental Engineering
University of Wollongong, NSW 2522 Australia



14th IACMAG 2014, Kyoto, Japan

CENTRE FOR GEOMECHANICS & RAILWAY ENGINEERING

UNIVERSITY OF WOLLONGONG

- Demand for freight and passenger transport has increased in the past decade.
- Increased traffic tonnage necessitates use of ground improvement techniques in Rail, Road and Port Infrastructure.

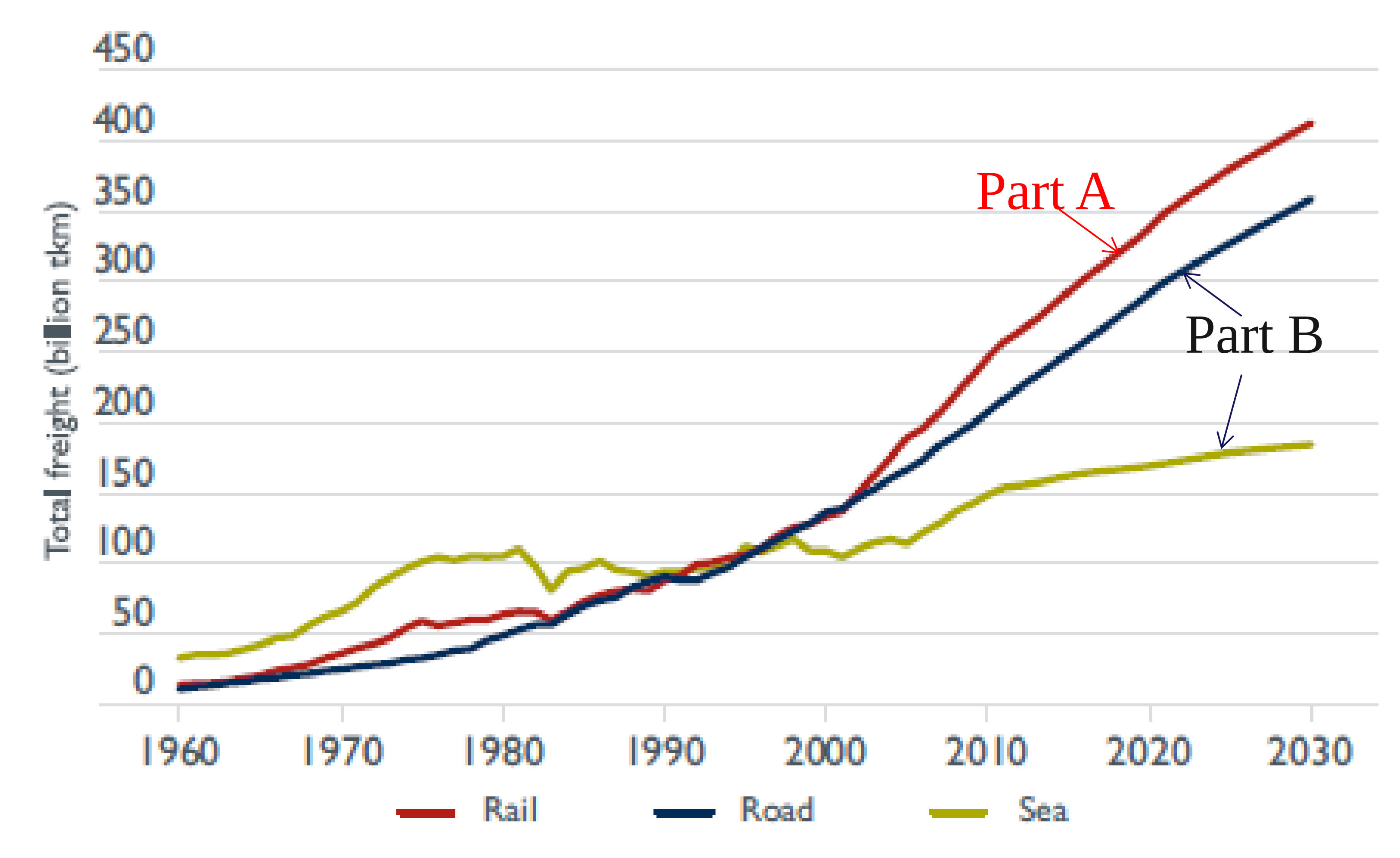

Figures from "Road and rail freight: competitors or complements?" Bureau of Infrastructure, Transport and Regional Economics, Australian Government Canberra.

PART A:
Railways – Granular media stabilisation

- Effect of confining pressure on track design
- DEM - Particle degradation modelling
- Cyclic loading and FEM modelling
- Track Contamination and design implications

Dynamic Process Simulation Test Facilities, Designed and Built at UoW

Prismoidal Triaxial Rig to Simulate a Track Section
(Specimen: 800x600x600 mm)

Cylindrical Triaxial Equipment
(Specimen: 300 mm dia.x600 mm high)

Effect of High Impact Loads and Track Degradation

Subgrade type	Location of shock mat	Ballast Breakage Index (BBI)
Without shock mat		
Stiff	-	0.170
Soft	-	0.080
With Shock mat		
Stiff	Above ballast	0.145
Stiff	Below ballast	0.129
Stiff	Above & below ballast	0.091
Soft	Above ballast	0.055
Soft	Below ballast	0.056
Soft	Above & below ballast	0.028

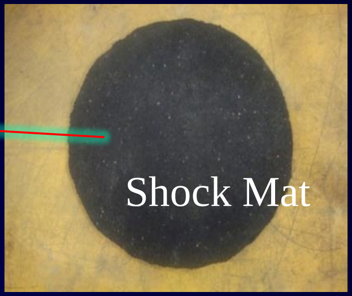

Nimbalkar, Indraratna, Dash & Christie (2012). JGGE, ASCE, Vol. 138(3), 281-294

Effect of Confining Pressure on Strain Behaviour of Ballast

(Indraratna, Lackenby and Christie (2005), Geotechnique, Vol. 55(4), 325-328)

Monotonic Loading

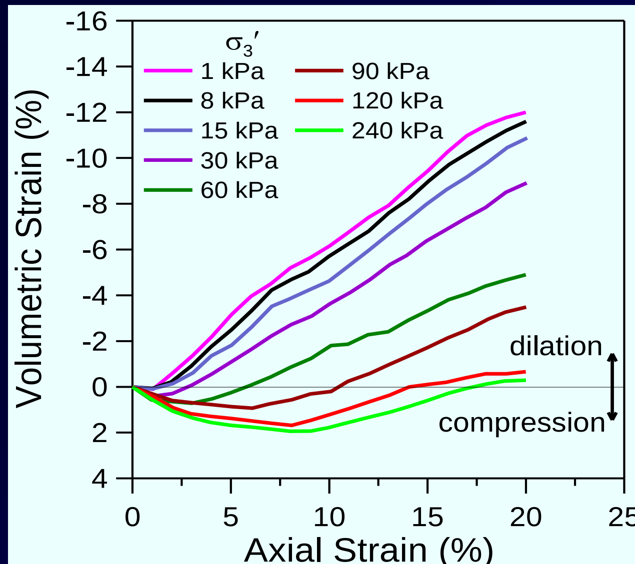

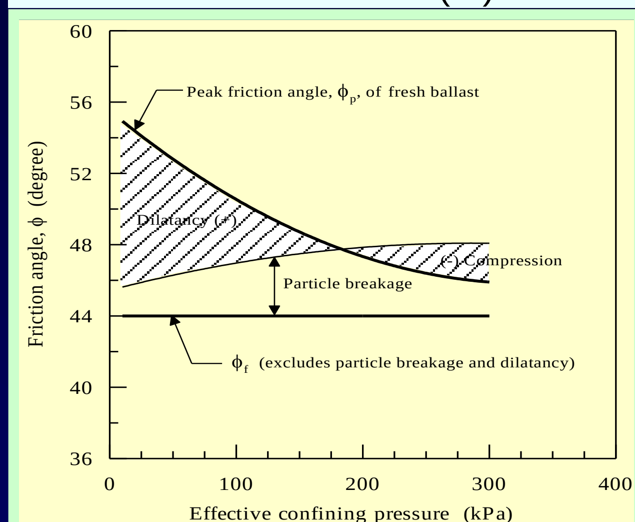

Cyclic Loading

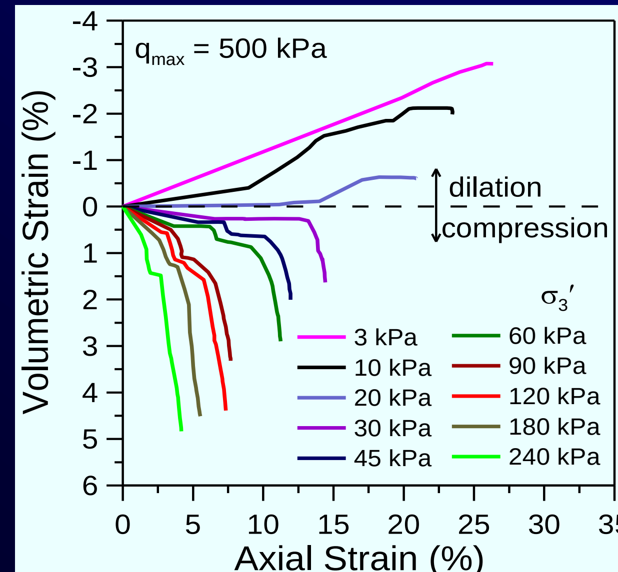

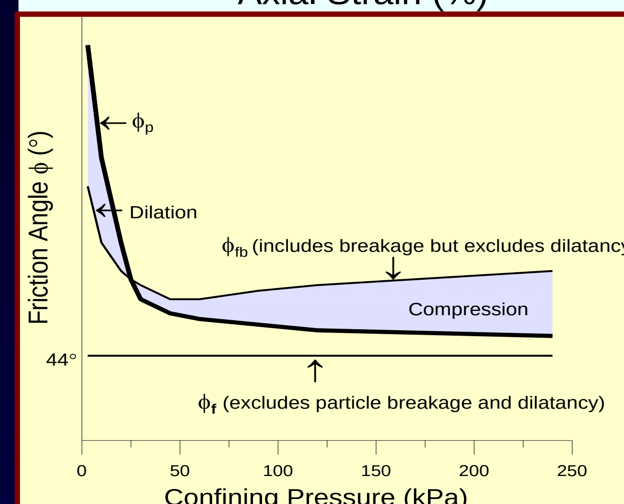

Increasing Confining Pressure using: Intermittent Lateral Restraints or Embedded Winged Sleepers

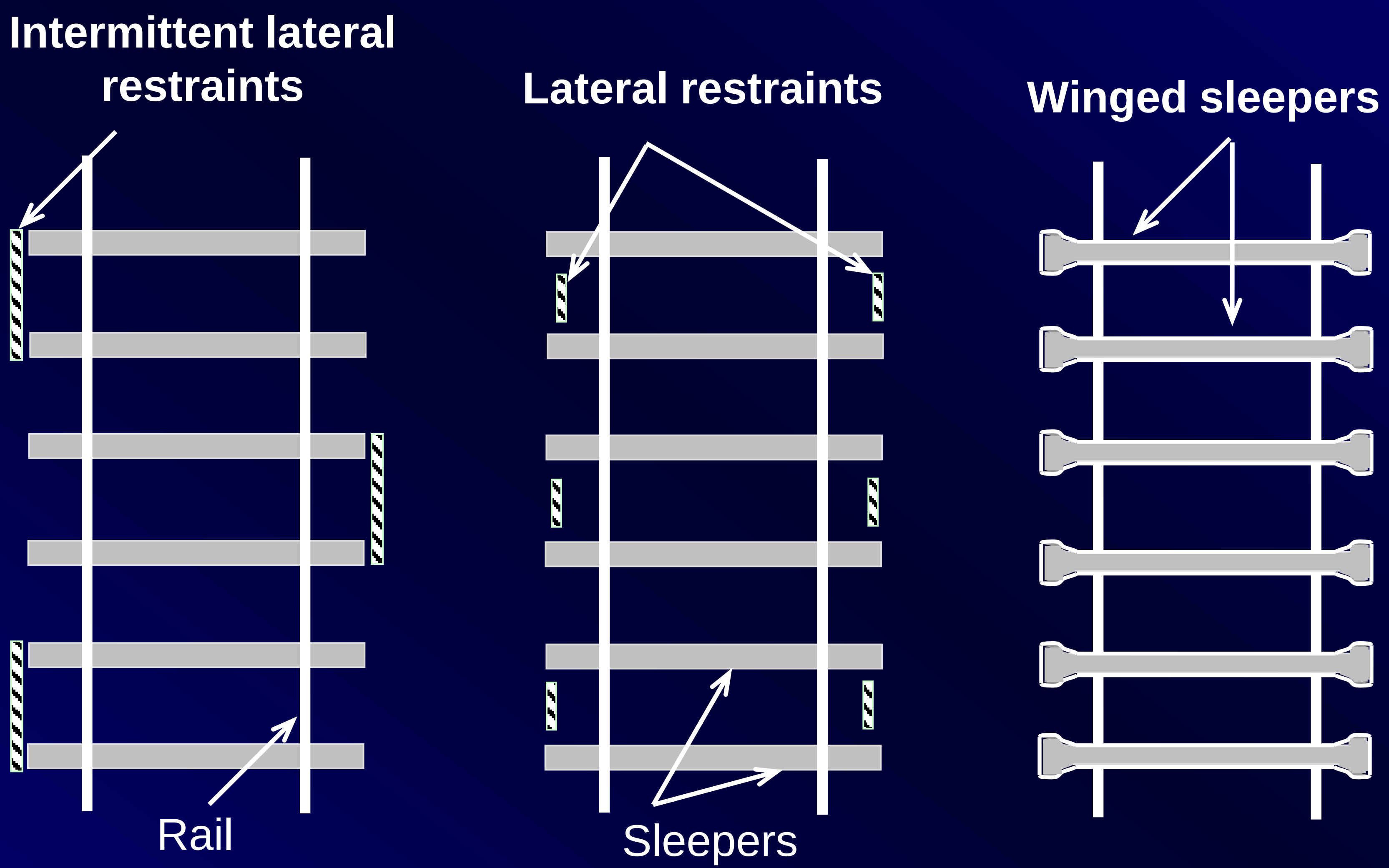

Lackenby, Indraratna, McDowell and Christie (2007) Geotechnique, ICE, UK. Vol. 57(6), 527-536

Effect of Confining Pressure on Particle Degradation (Cyclic Loading)

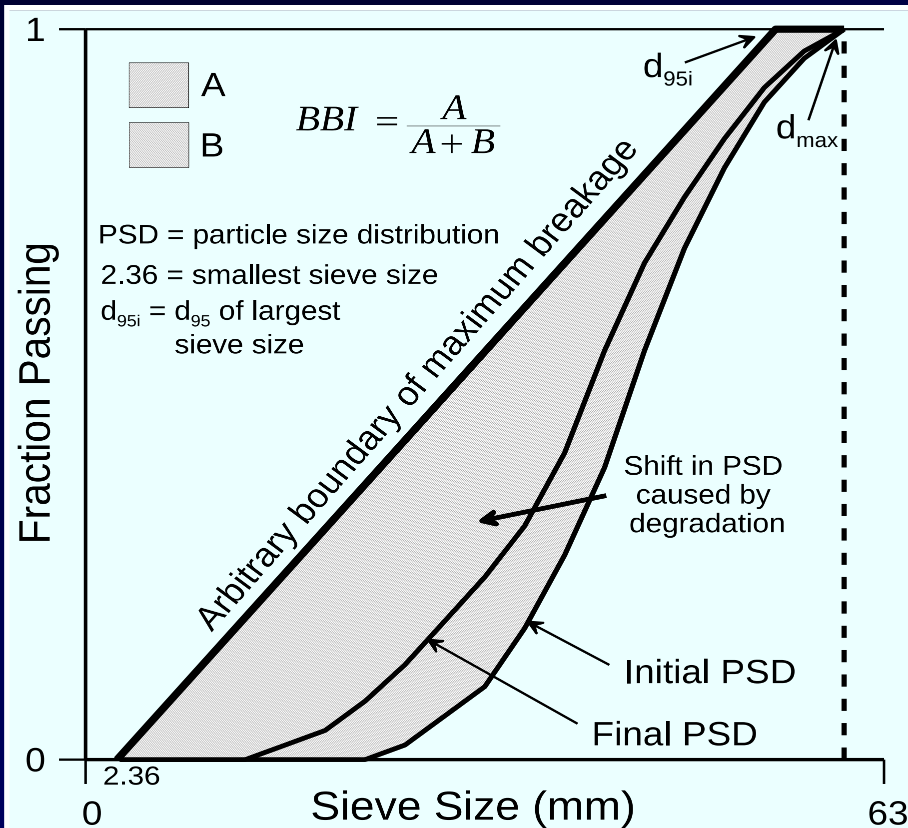

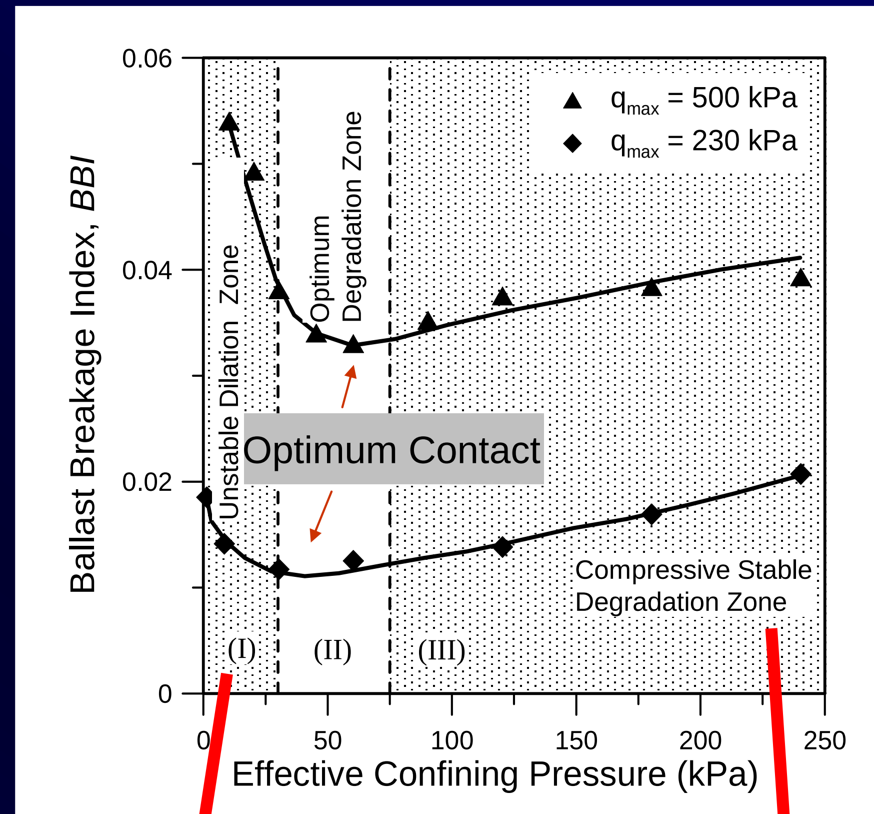

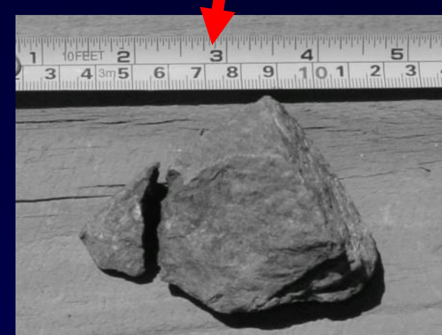

Ballast Breakage Index (BBI)

Indraratna, Lackenby and Christie (2005) Geotechnique, Vol. 55(4), 325-328

Constitutive Modelling Incorporating Ballast Breakage – Energy Approach

dE_B = increment of energy consumption due to particle breakage

$$\frac{q}{p} = \frac{\left(1-\frac{d\varepsilon_v}{d\varepsilon_1}\right)\tan^2\left(45^\circ+\frac{\phi_f}{2}\right)-1}{\left[\frac{2}{3}+\frac{1}{3}\left(1-\frac{d\varepsilon_v}{d\varepsilon_1}\right)\tan^2\left(45^\circ+\frac{\phi_f}{2}\right)\right]} + \frac{dE_B/d\varepsilon_1\left(1+\sin\phi_f\right)}{p\left[\frac{2}{3}+\frac{1}{3}\left(1-\frac{d\varepsilon_v}{d\varepsilon_1}\right)\tan^2\left(45^\circ+\frac{\phi_f}{2}\right)\right]}$$

Conventional theory

p = Effective mean stress

q = Deviator stress

ϕ_f = basic friction angle

Indraratna and Salim (2002) Geotechnical Engineering, ICE Proceedings, UK.

Constitutive Modelling of Particle Breakage

Salim & Indraratna (2004), Canadian Geotechnical Journal, Vol. 41(4), 657-671

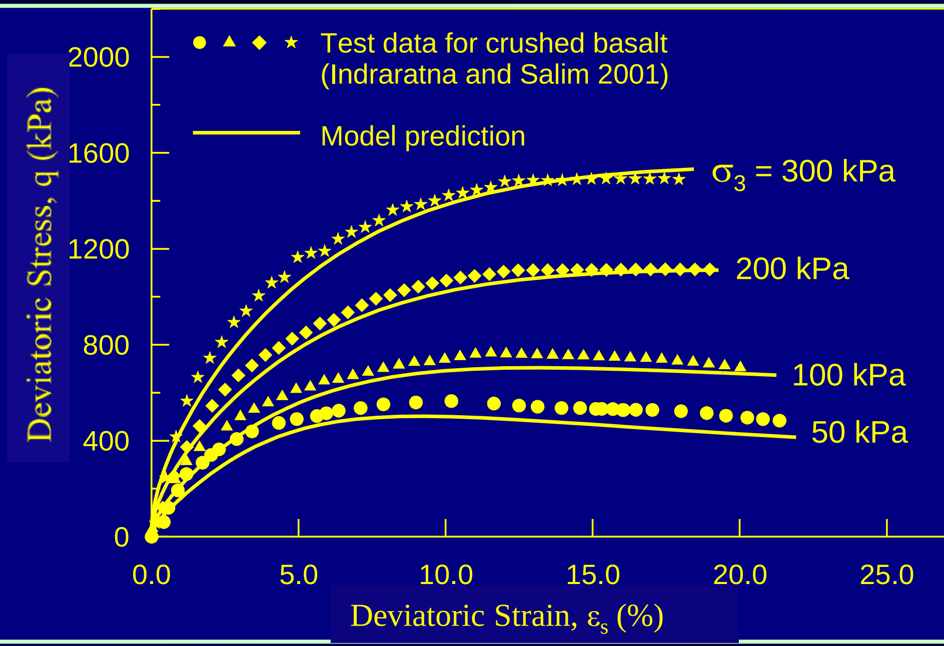

Stress-Strain behaviour

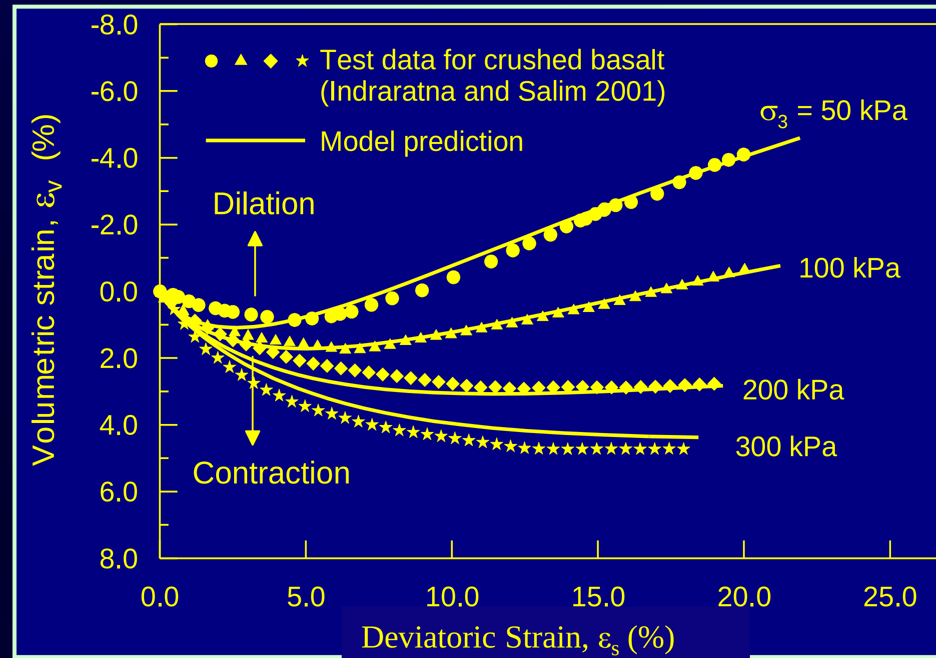

Volume Change Behaviour

$$d\varepsilon_s^p = \frac{2\alpha\kappa\left(\frac{p}{p_{cs}}\right)\left(1-\frac{p_{o(i)}}{p_{cs(i)}}\right)\left(9+3M-2\eta^* M\right)\eta\, d\eta}{M^2\left(1+e_i\right)\left(\frac{2p_o}{p}-1\right)\left[9\left(M-\eta^*\right)+\frac{B}{p}\left\{\chi+\mu\left(M-\eta^*\right)\right\}\right]}$$

$$\frac{d\varepsilon_v^p}{d\varepsilon_s^p} = \frac{9\left(M-\eta\right)}{9+3M-2\eta^* M} + \left(\frac{B}{p}\right)\left[\frac{\chi+\mu\left(M-\eta^*\right)}{9+3M-2\eta^* M}\right]$$

Model Parameters need to be determined by large-scale testing

Distinct Element Modelling: Train Velocity vs Breakage

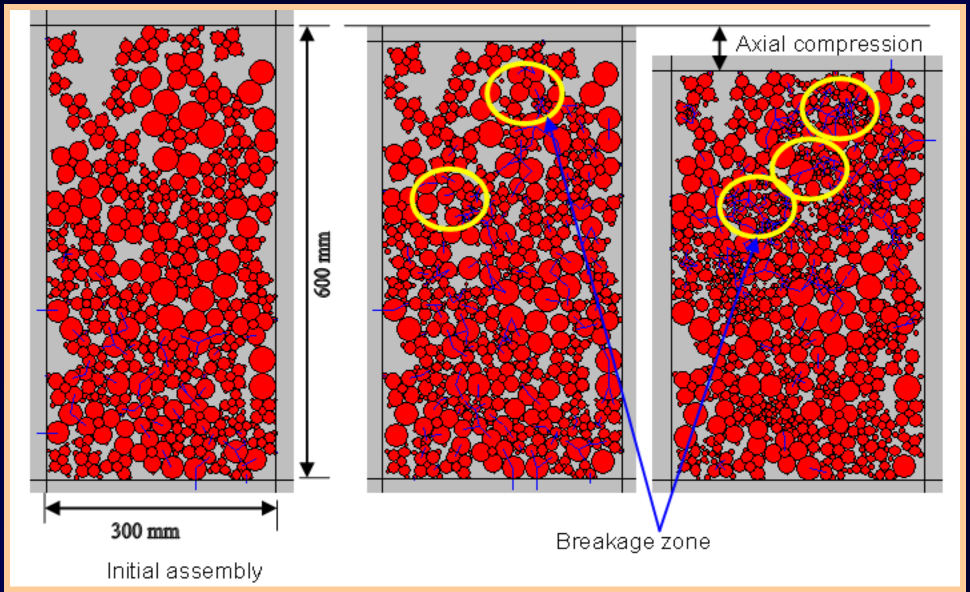

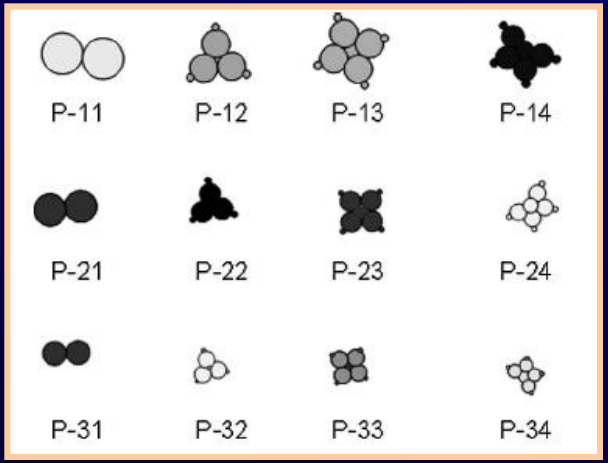

Model particle shapes and sizes

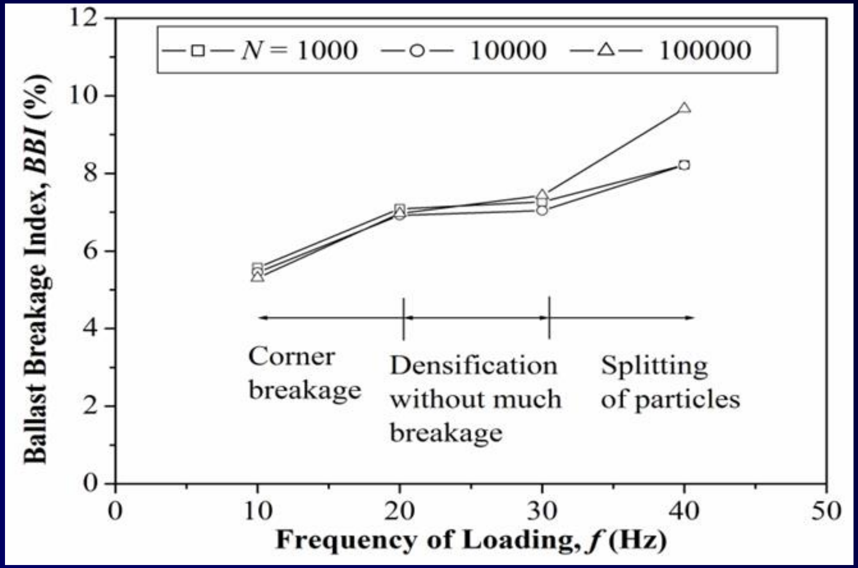

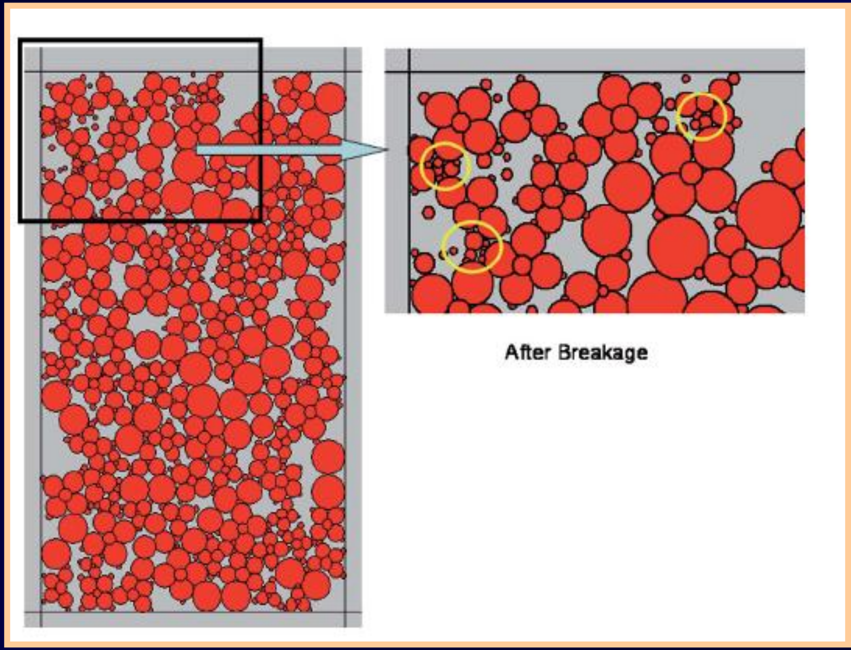

Particle Breakage near the top plate

Hossain, Indraratna, Darve, & Thakur (2007). Geomech & Geoengg, Vol. 2(3), 175-181

Constitutive model: Critical State capturing particle breakage

Indraratna, B., Sun, Q. D. & Nimbalkar, S. (2014). *Can. Geotech. J.* in press.

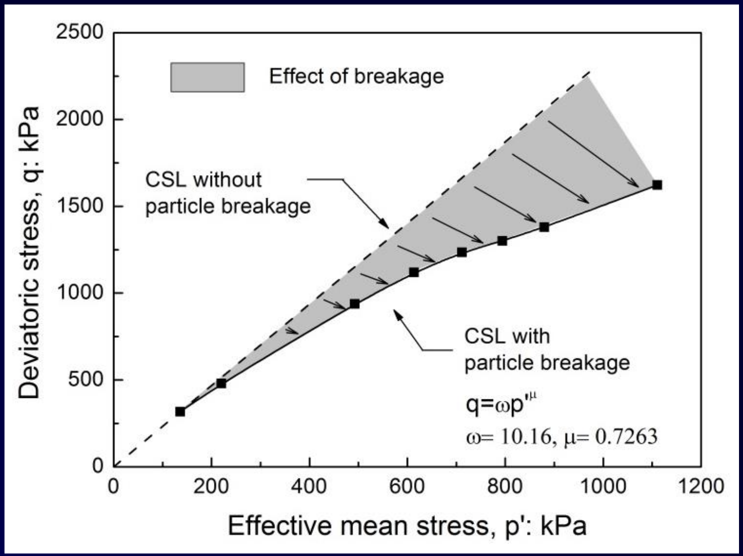

$$M_c = M_{c0} - \left[1 - exp\left(-\alpha \cdot BBI\right)\right]$$

M_{c0} is critical state stress ratio for BBI = 0

$$\upsilon_c = \Gamma_{ref} - a \cdot exp\left(b \cdot BBI\right) - \lambda \ln p'$$

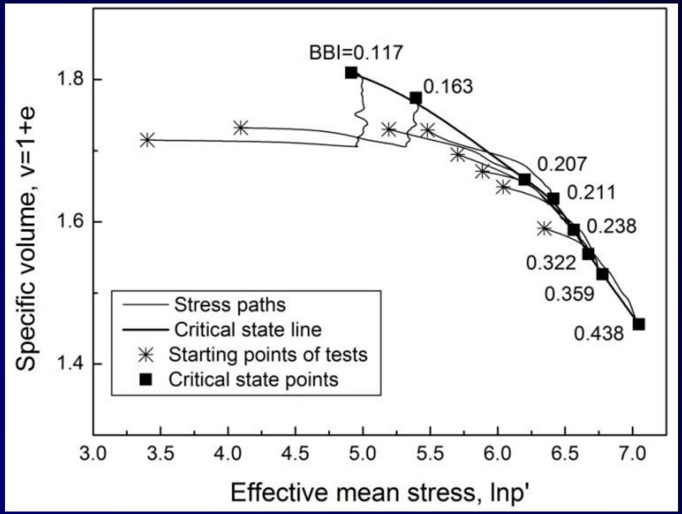

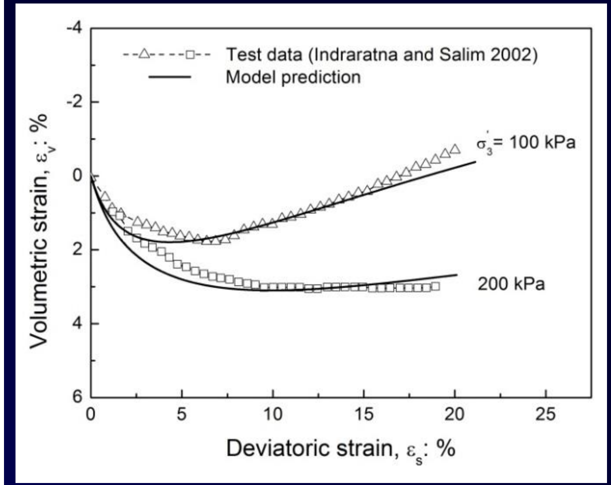

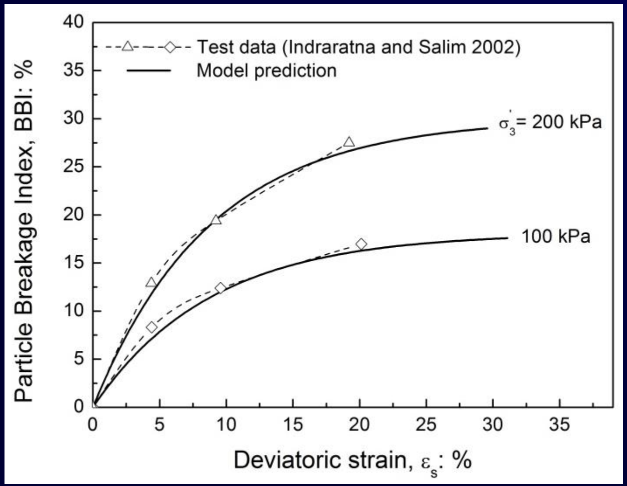

DEM Modelling Geogrid-reinforced Ballast under Shearing Loads

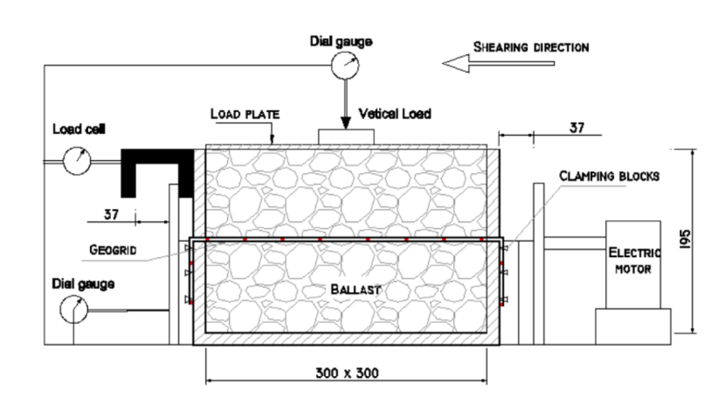

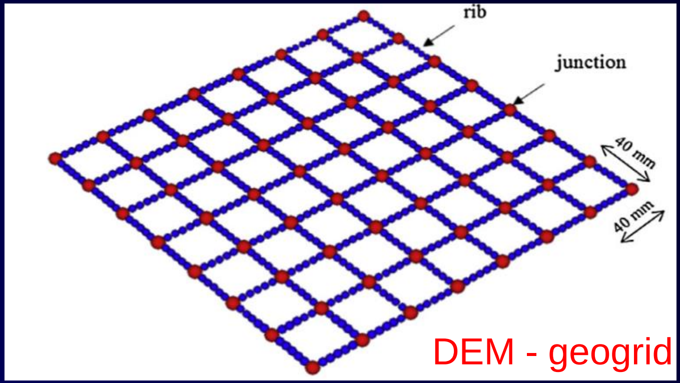

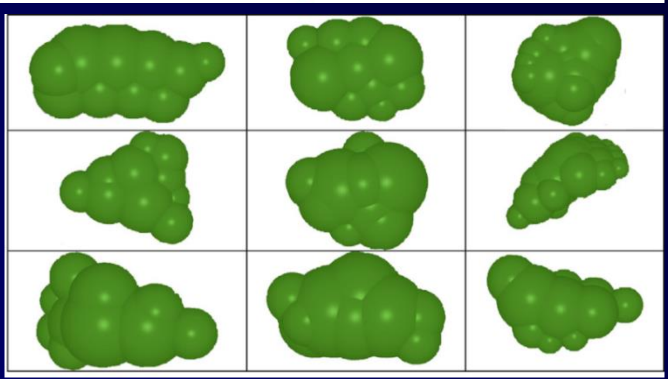

DEM particle shapes and sizes

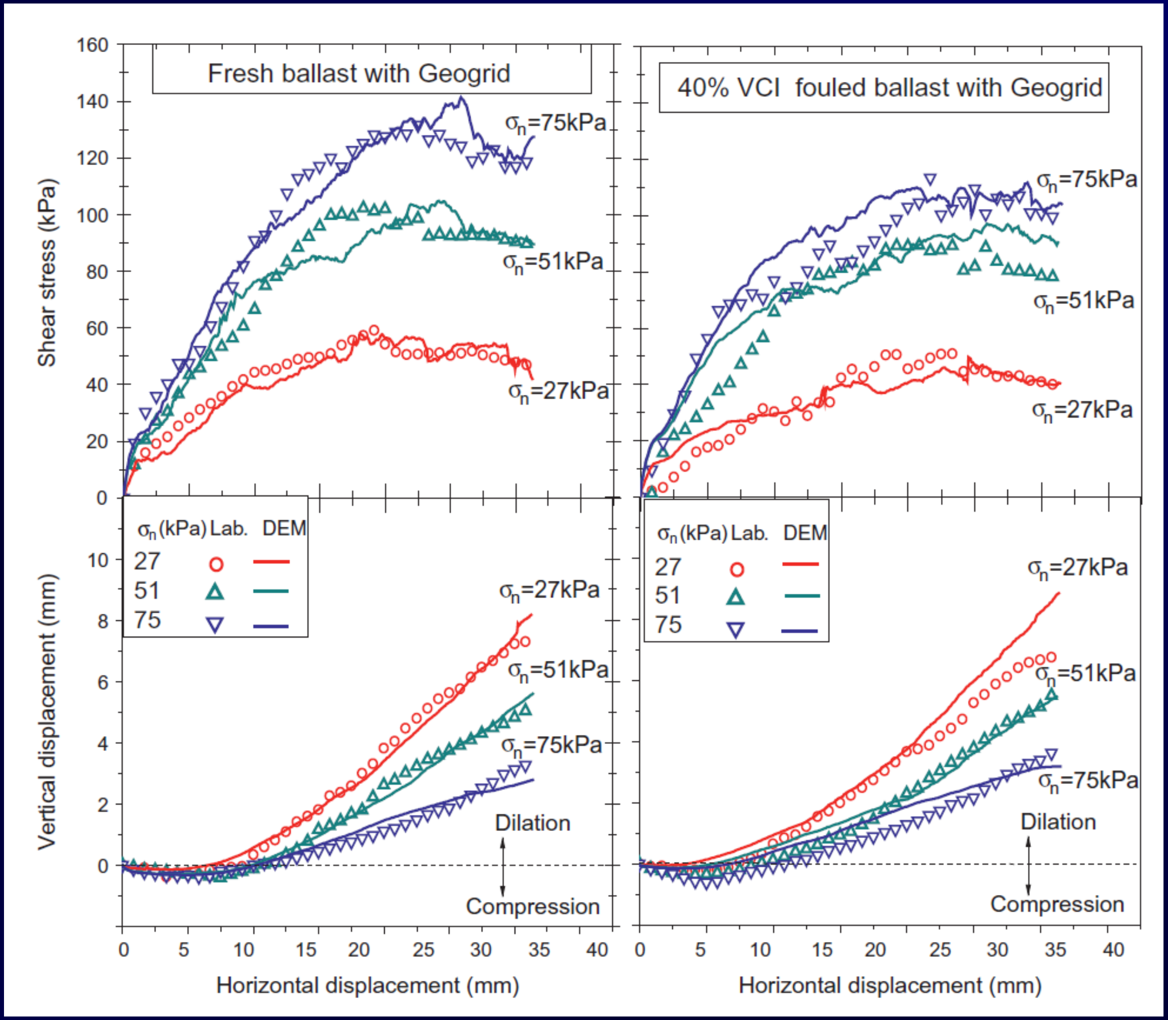

Comparison of shear stress and displacements for DEM simulation of reinforced ballast

Ngo, Indraratna, and Rujikiatkamjorn (2014). Computers & Geotechnics, Vol. 55, 224-231

DEM Model for Geogrid-reinforced Ballast under Direct Shearing

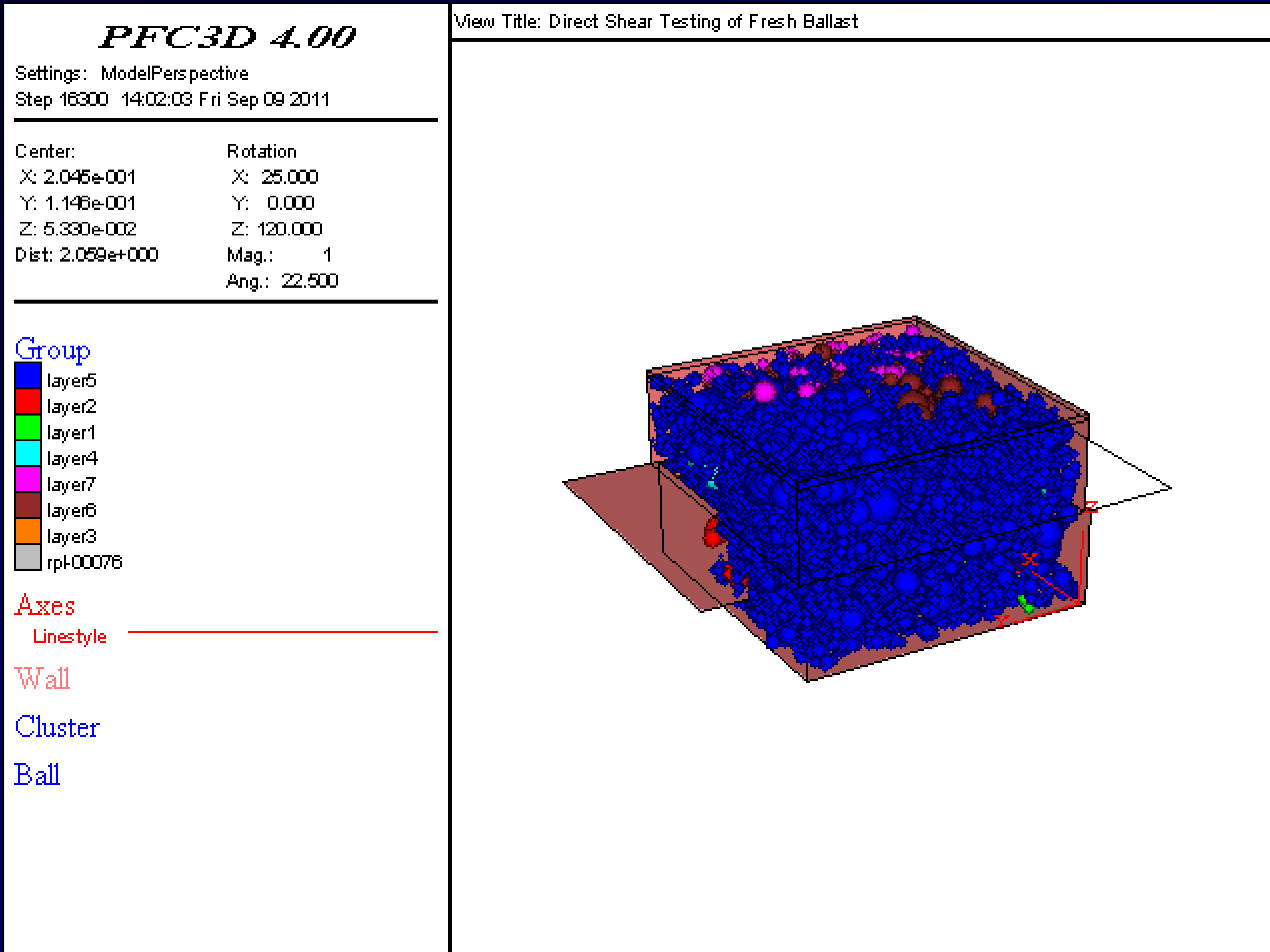

Role of Ballast Fouling on Track Performance

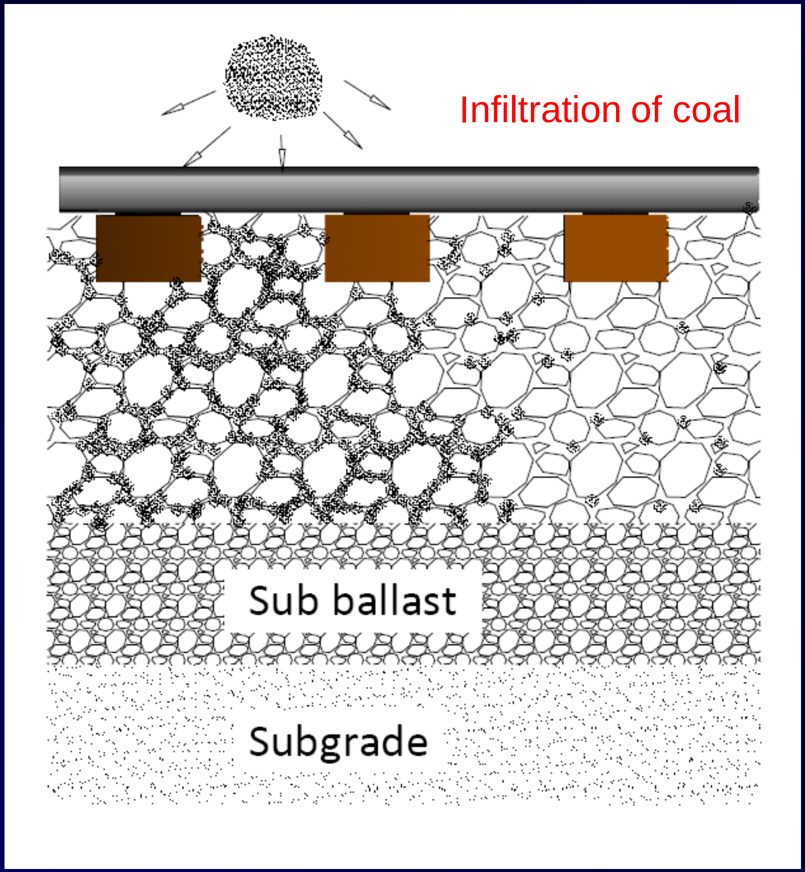

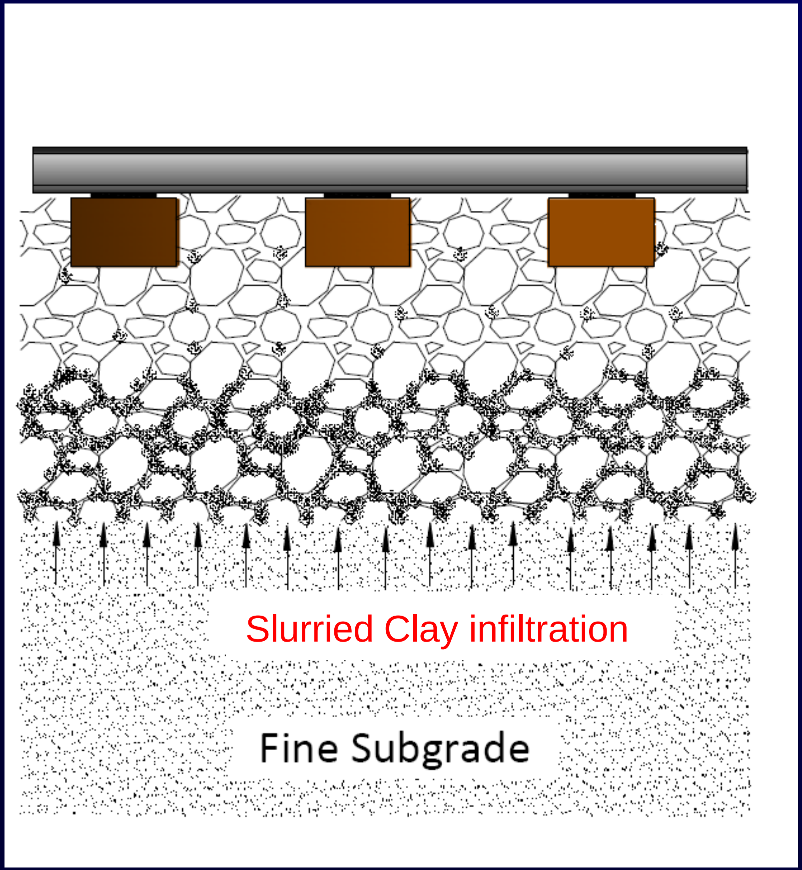

Void Contaminant Index (VCI) proposed by UOW

$$VCI = \frac{(1+e_f)}{e_b} \times \frac{G_{s.b}}{G_{s.f}} \times \frac{M_f}{M_b} \times 100$$

e_b = Void ratio of clean ballast

e_f = Void ratio of fouling material

$G_{s\text{-}b}$ = Specific gravity of clean ballast

$G_{s\text{-}f}$ = Specific gravity of fouling material

M_b = Dry mass of clean ballast

M_f = Dry mass of fouling material

Bounding Surface Model for Fouled Ballast (Indraratna et al., 2014; Geotechnique, in press)

Bounding Surface

$$F = \bar{q} - \alpha\left(\sqrt{p_a/p'_o}\right) M\,\bar{p}' \left[\frac{\ln(\bar{p}'_c/\bar{p}')}{\ln R}\right]^{1/N} = 0$$

Non-Associated Flow rule

$$\frac{d\varepsilon_v^p}{d\varepsilon_q^p} = M_f - \eta$$

$M_f = f(VCI)$

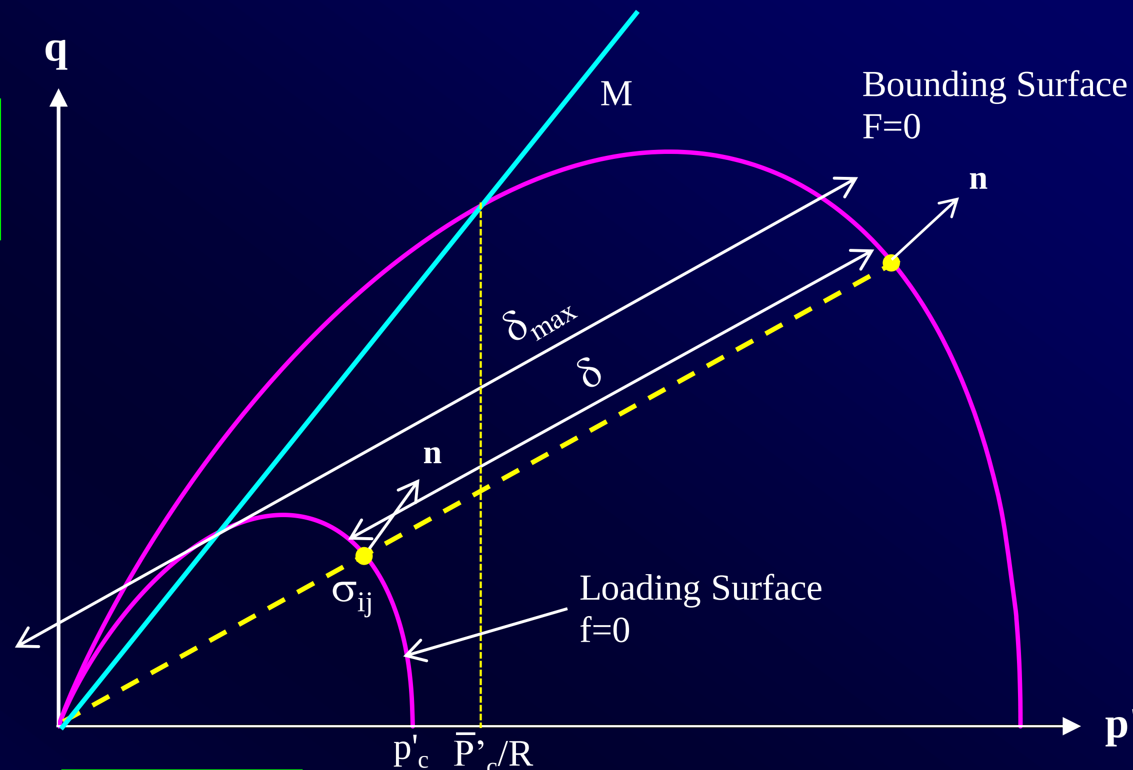

Hardening modulus

$$h = h_b + h_f$$

$$h_b = \frac{M\alpha\left(\sqrt{p_a/p'_o}\right)\bar{p}\left[\frac{\ln\left(\bar{p}'_c/\bar{p}\right)}{\ln R}\right]^{1/N}}{N\bar{p}'_c \ln\left(\bar{p}'_c/\bar{p}\right)} \times \frac{(1+e_o)}{(\lambda-\kappa)}\bar{p}'_c \times \frac{m_p}{\left\|\partial F/\partial\bar{\sigma}\right\|}$$

$$h_f = \left\{\frac{1}{\bar{p}_c}\frac{\partial \bar{p}'_c}{\partial \varepsilon_v^p}\left(\frac{\delta}{\delta_{max}-\delta}\right)\right\} f\,(VCI)$$

Impeded Track Drainage due to Ballast Fouling

Large-scale permeability test apparatus

Hydraulic Conductivity (k) of fouled ballast

$$k = \frac{k_b \times k_f}{k_f + {VCI}/{100} \times (k_b - k_f)}$$

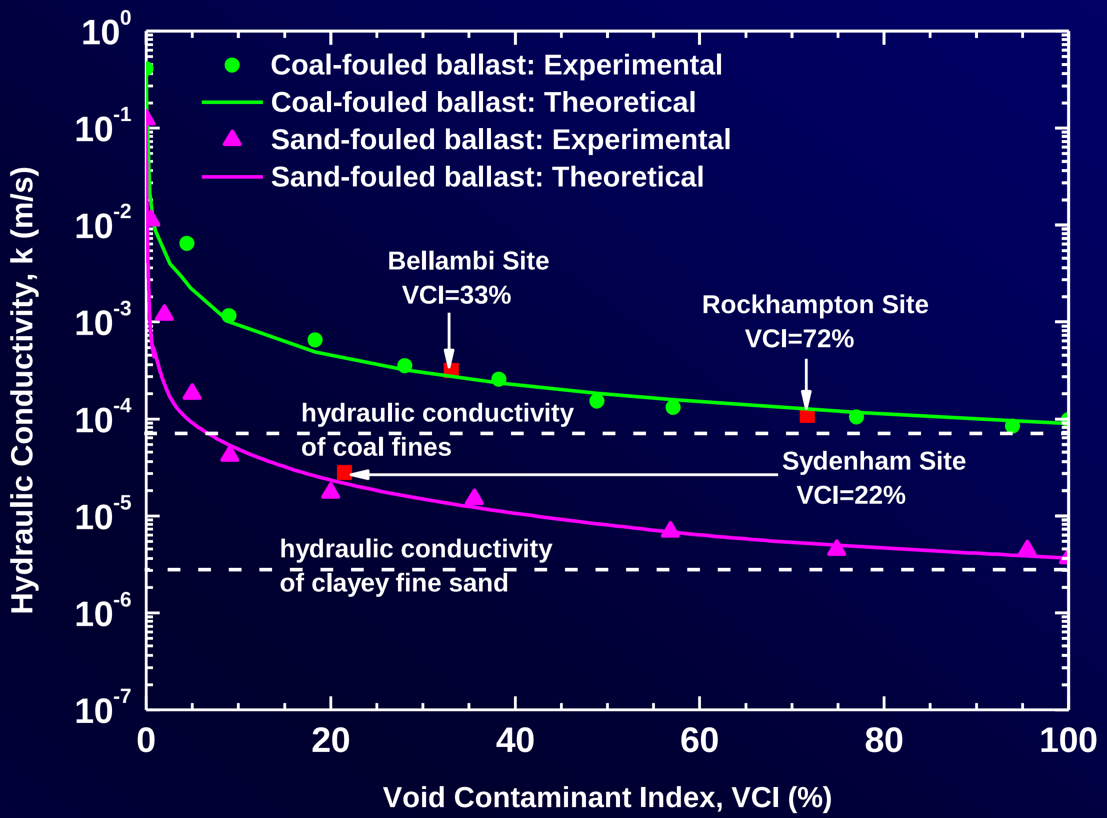

Variation of hydraulic conductivity vs. Void Contaminant Index

Tennakoon, Indraratna, Cholachat, Nimbalkar and Neville (2012) ASTM Geotechnical Testing Journal, Vol. 35(4), 1-12

k_b = Hydraulic conductivity of clean ballast

k_f = Hydraulic conductivity of fouling material

Cyclic loading (sinusoidal form) of Track

- Initial static loading to reach the minimum cyclic deviator stress.
- Frequency conditioning phase (f = 1 Hz, N = 10) to prevent any loss of actuator contact with the specimen.
- Cyclic loading phase (f = 5, 10, 20 and 40 Hz, N = 500 000).

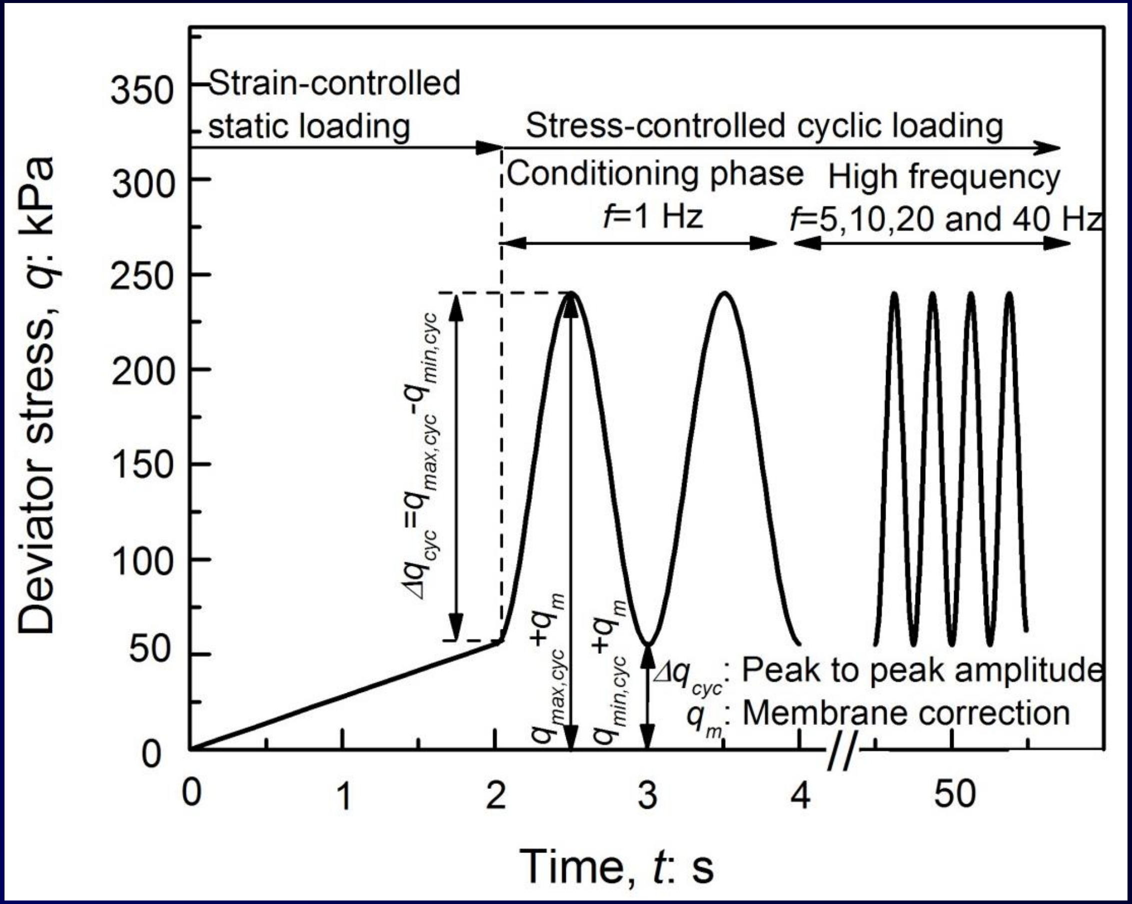

Effect of frequency on the axial strain of ballast

Sun, Q. D., Indraratna, B. & Nimbalkar, S. (2014). *Géotechnique*, doi: 10.1680/geot./14-T-015.

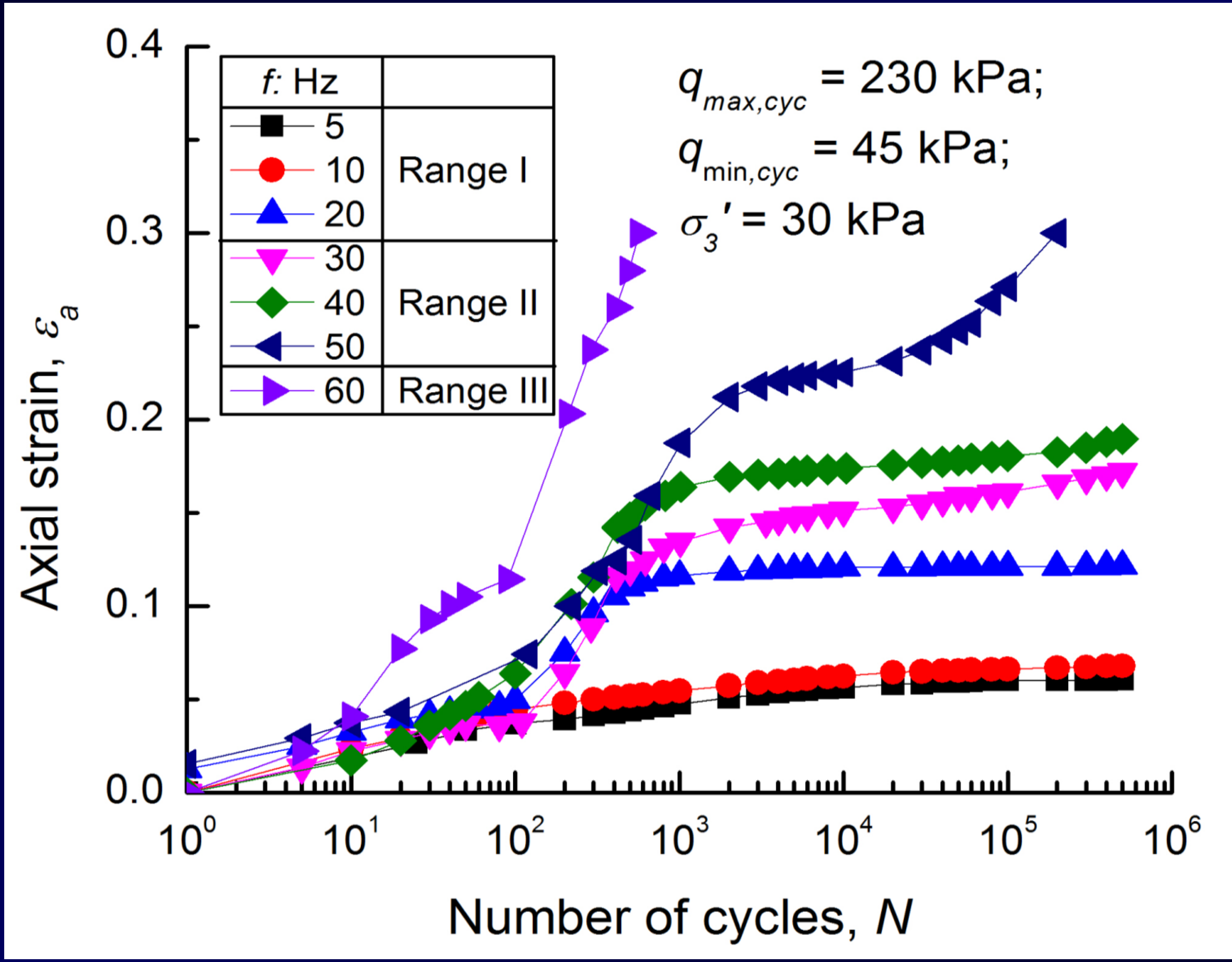

Range I: Plastic shakedown (5Hz ≤ f ≤ 20 Hz)

Range II: Plastic shakedown followed by Ratcheting (30 Hz ≤ f ≤ 50 Hz)

Range III: Plastic collapse (f = 60 Hz)

Field Trial on Instrumented Track in Bulli and Singleton

Geocomposite layer (geogrid+geotextile) before ballast placement

Ballast placement over the geocomposite

Geogrid layer placed above the capping

Settlement pegs placement in the track

Field Instrumentation - Bulli

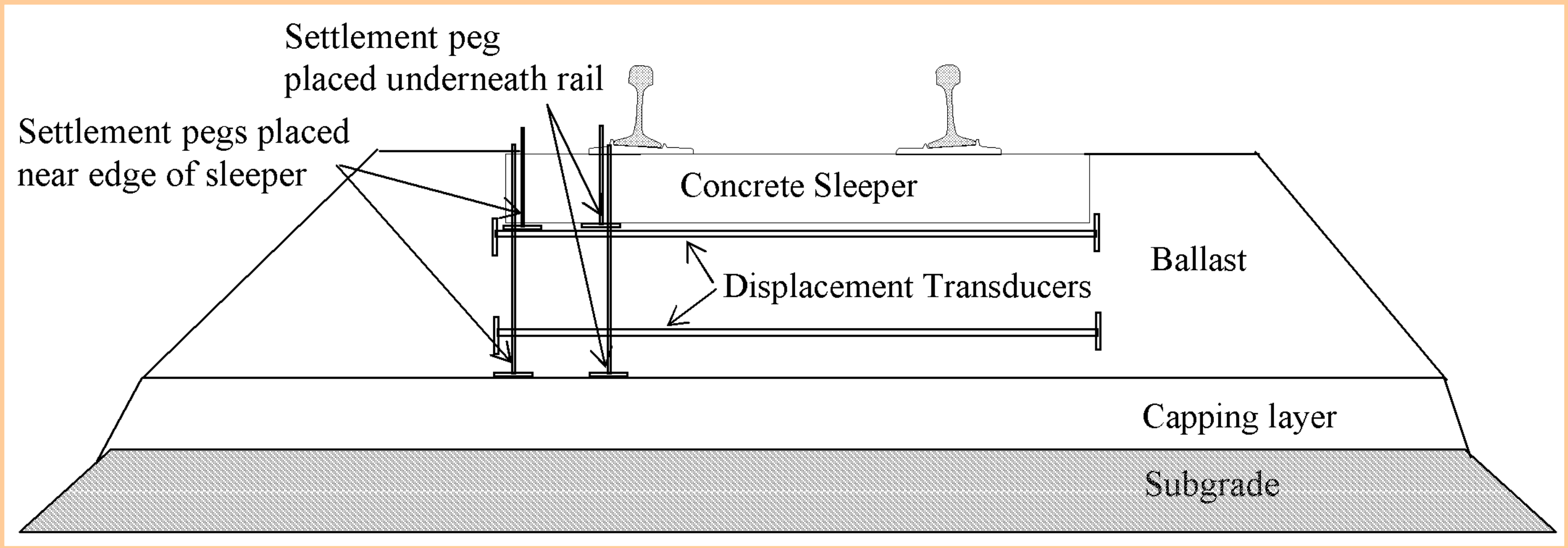

Settlement pegs installed at ballast-capping interface

Displacement transducers installed at sleeper-ballast interface

Field Deformation Response

Indraratna et al. (2010). JGGE, ASCE, Vol. 136(7), 907-917

Indraratna et al. (2014). ICE Proc. Ground Improvement, Vol. 167(1), 24-34

Bulli Track

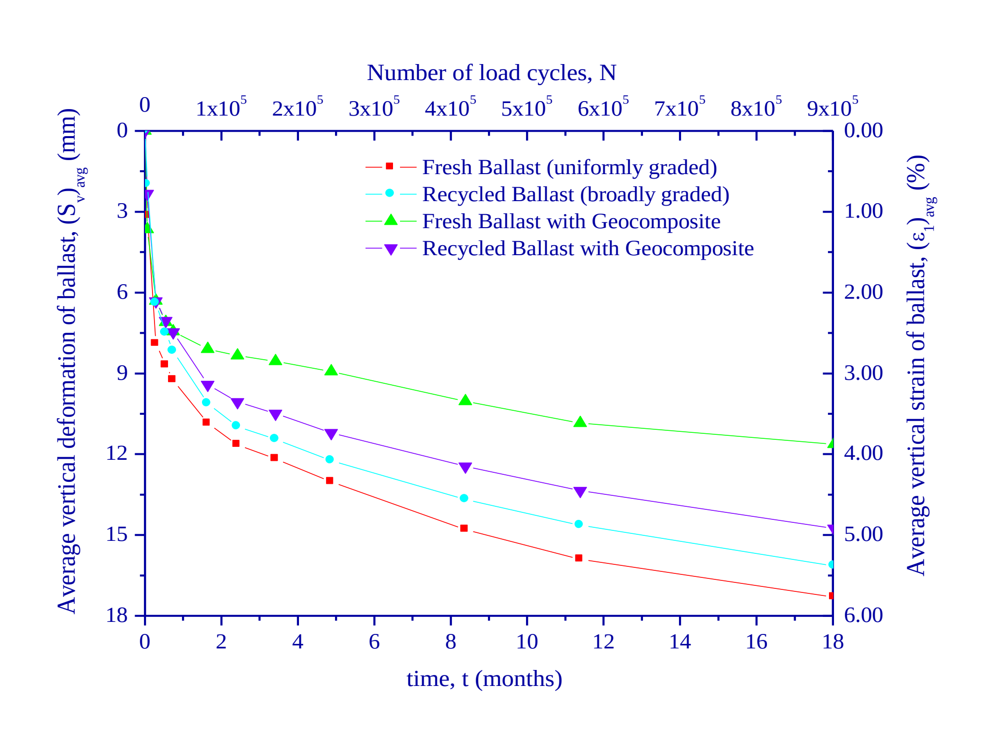

The recycled ballast performed well because, it was broadly graded compared to the relatively uniform fresh ballast.

Singleton Track

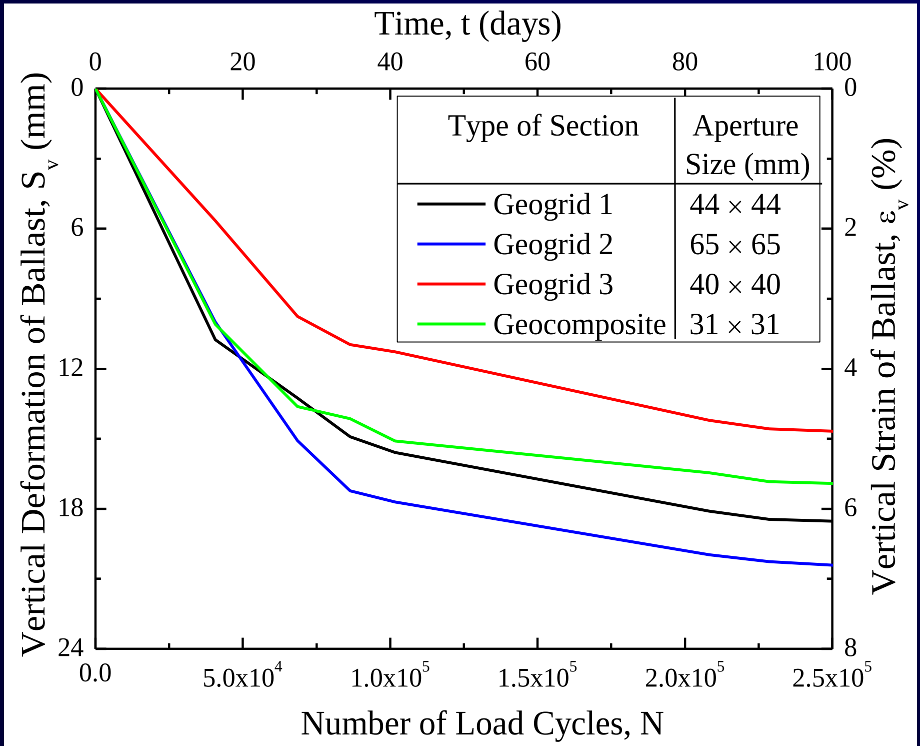

Optimum aperture size of geogrids is about $1.15D_{50}$ of ballast.

Plane Strain FEM Analysis of Track Substructure (Confining Pressure @ 50 kPa by geocells)

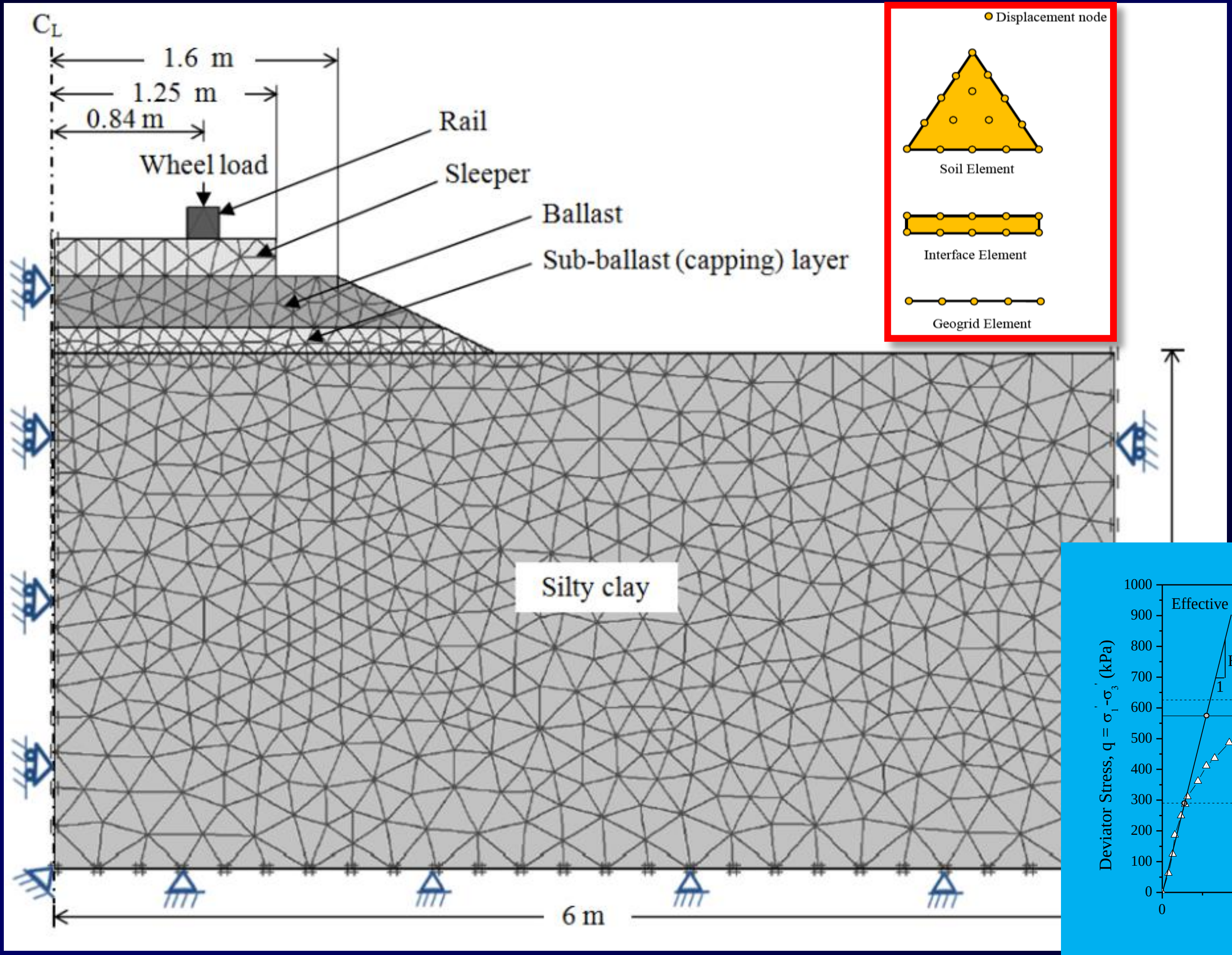

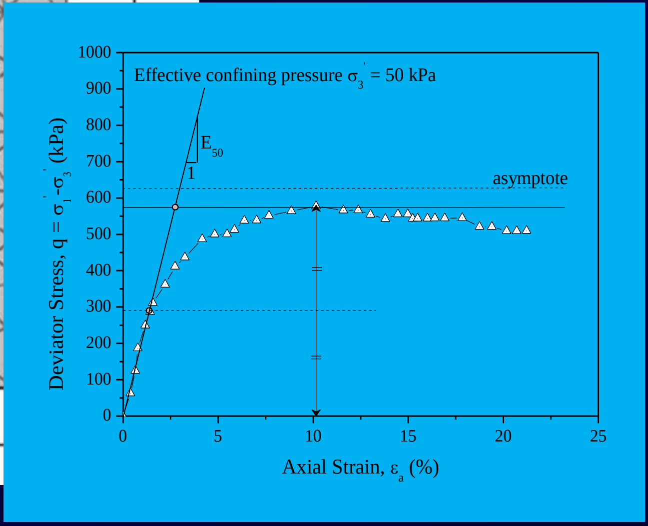

Track transverse section deformation

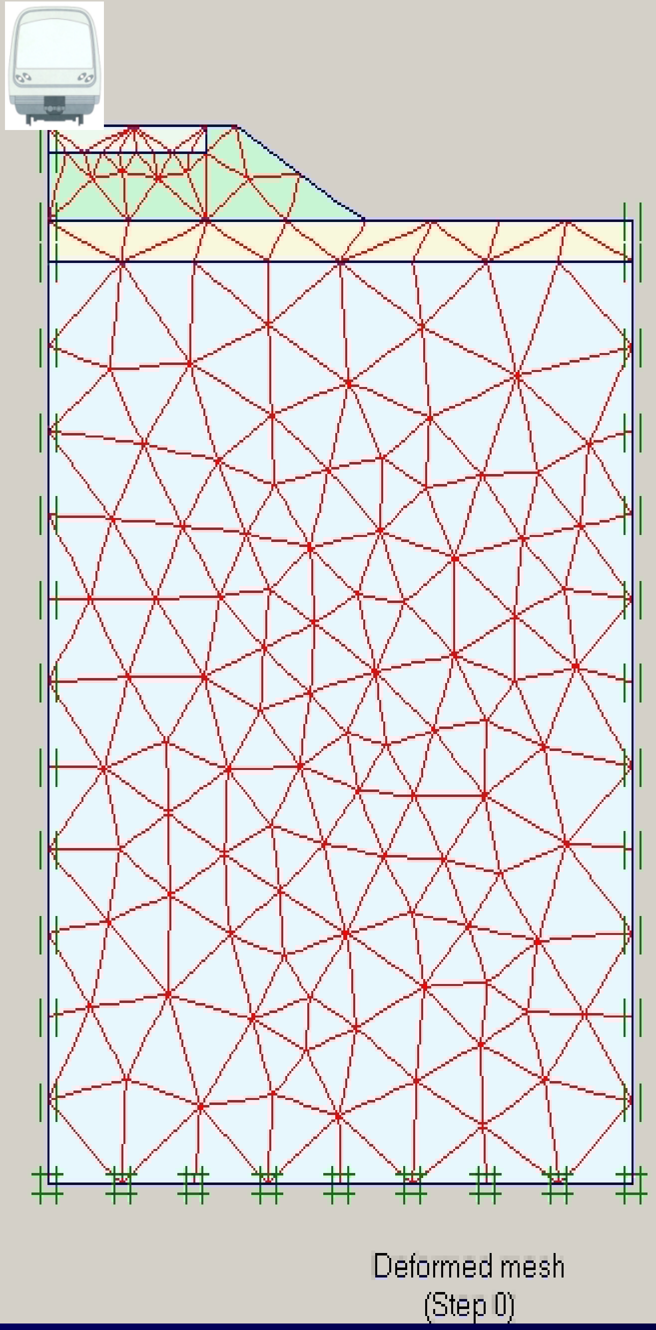

Track longitudinal section deformation

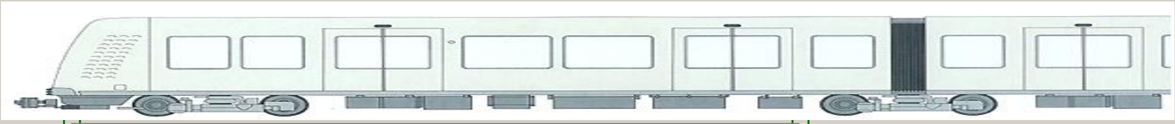

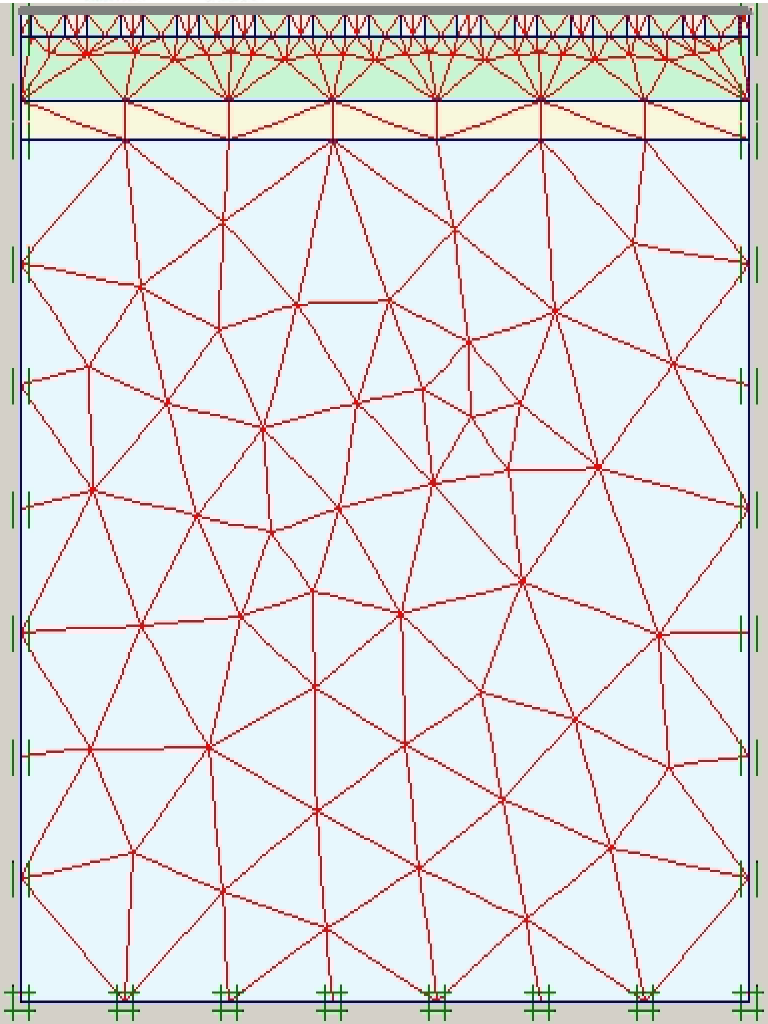


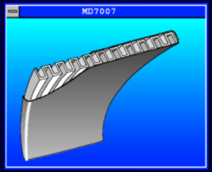
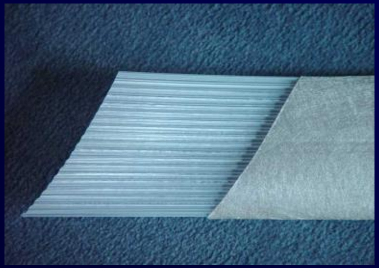


PART B:
Road Embankments and Port Reclamation – Soft Soil Stabilisation

- Concepts of vacuum consolidation
- Factor affecting vacuum consolidation
- 2D and 3D FEM modelling of vacuum consolidation

Membrane-type Vacuum Application (Courtesy Austress-Menard)

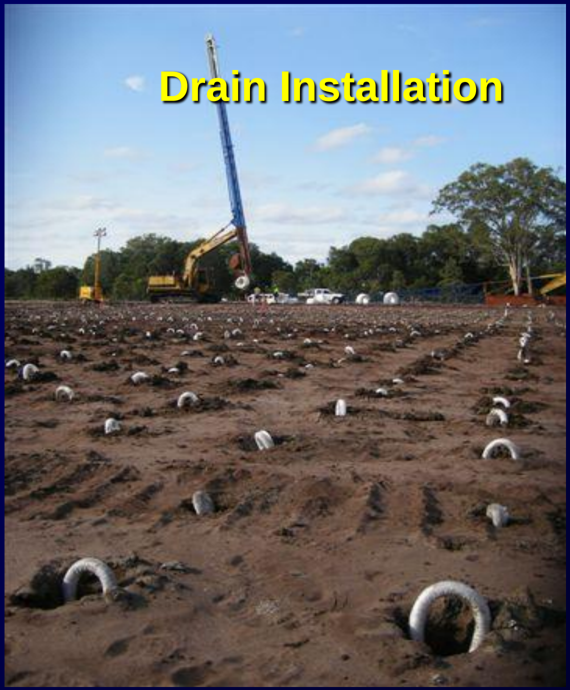

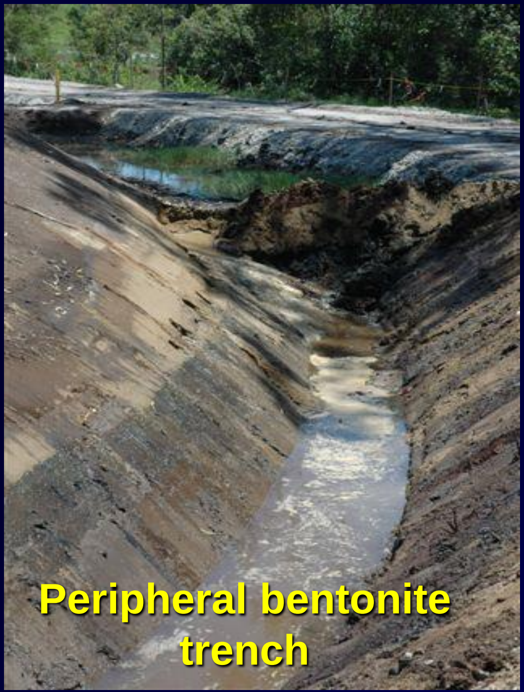

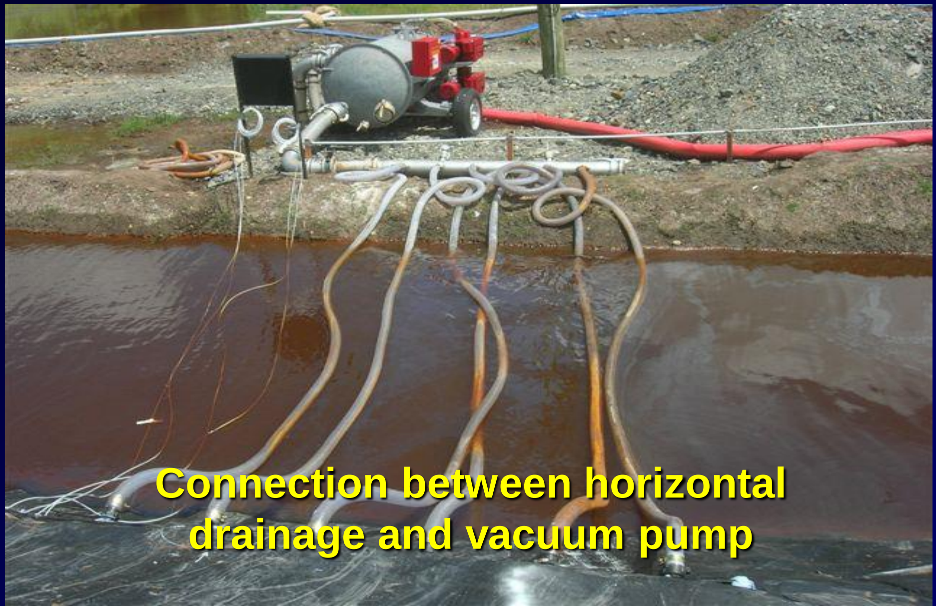

Principle of Vacuum Consolidation

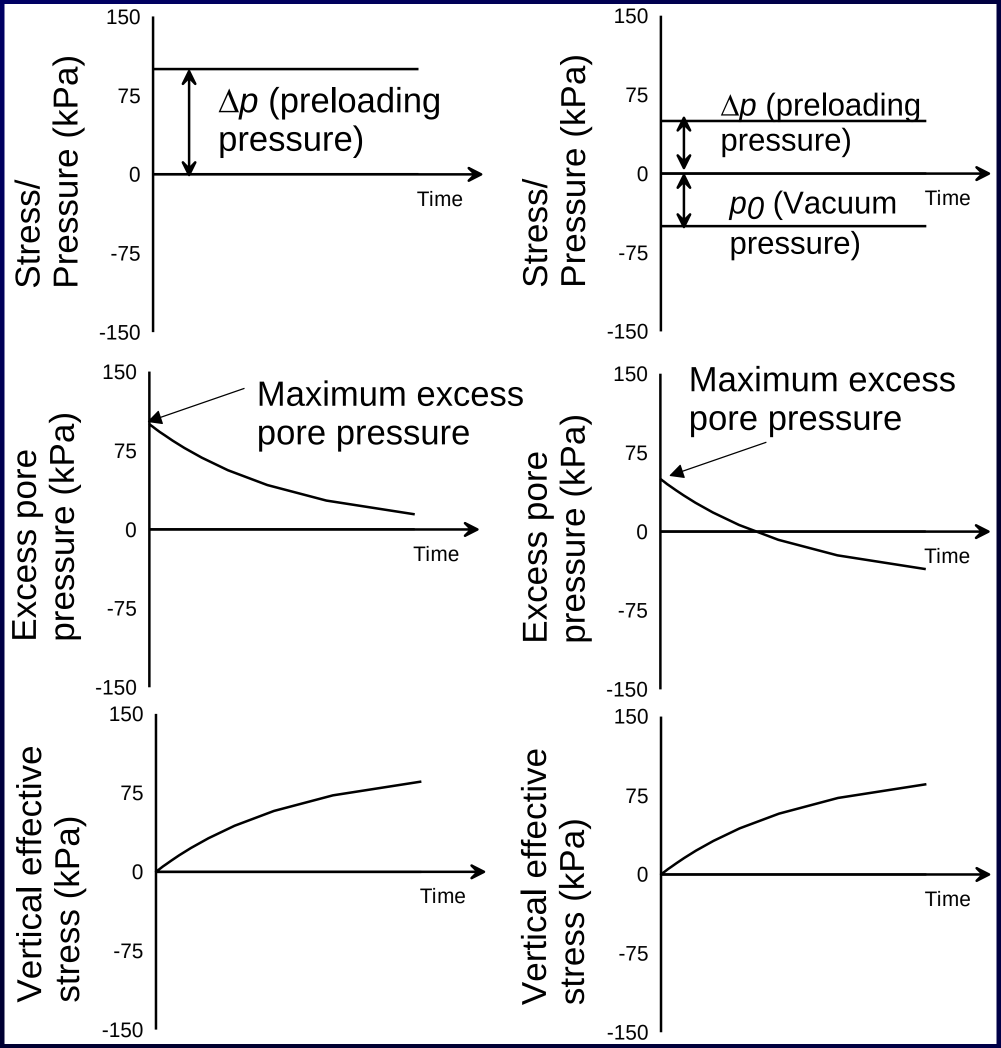

Consolidation: (a) conventional surcharge loading; (b) idealised vacuum preloading (Indraratna et al. 2005).

Governing Equation

$$c_h\left(\frac{1}{r}\frac{\partial u}{\partial r}+\frac{\partial^2 u}{\partial r^2}\right)+c_v\frac{\partial^2 u}{\partial z^2}=\frac{\partial u}{\partial t}$$

VP directly adjusts the initial pore pressure boundary conditions.

Vertical consolidation term can be ignored if Z is very large.

Pore Pressure generation and retarded dissipation within the Smear Zone

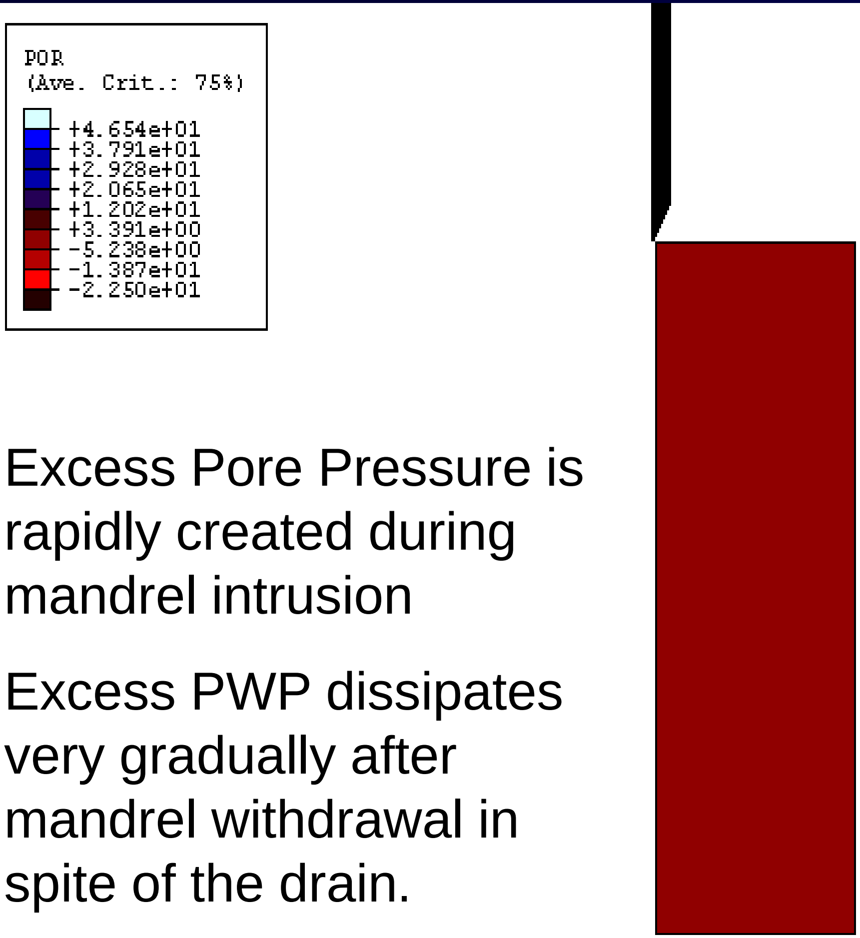

Excess Pore Pressure is rapidly created during mandrel intrusion

Excess PWP dissipates very gradually after mandrel withdrawal in spite of the drain.

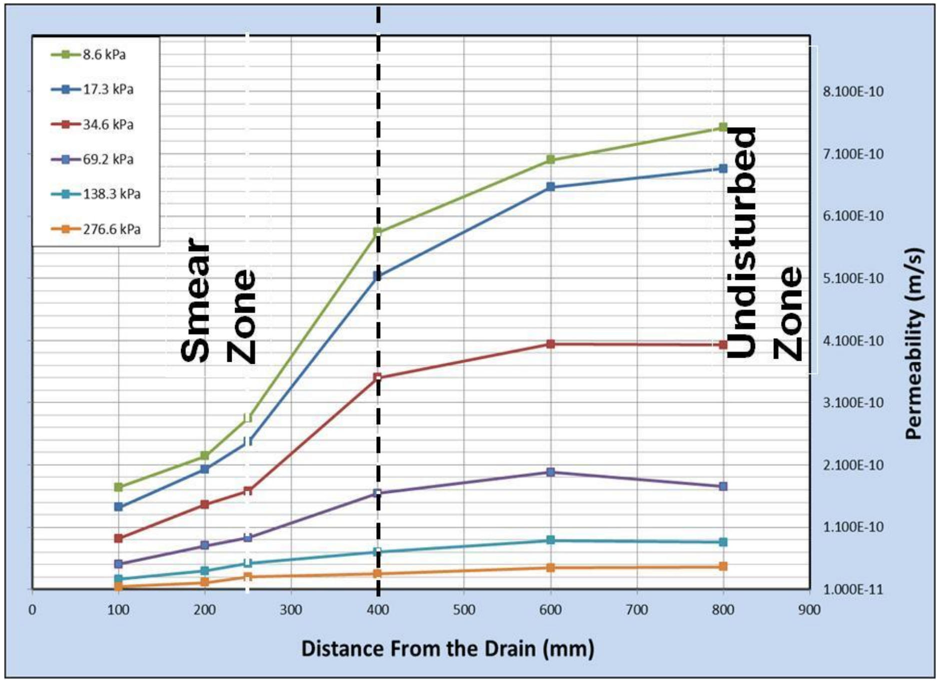

Mandrel Driving INCREASES effective vertical stress, hence, the lateral permeability decreases within the smear zone (Sathananthan, Indraratna, & Rujikiatkamjorn (2008), ASCE J. of Geomechanics, Vol. 8(6), 355-365).

Analytical and Numerical Simulation
Multi-drain Analysis and Plane Strain Conversion

Field condition: Axisymmetric

2D plane strain FEM

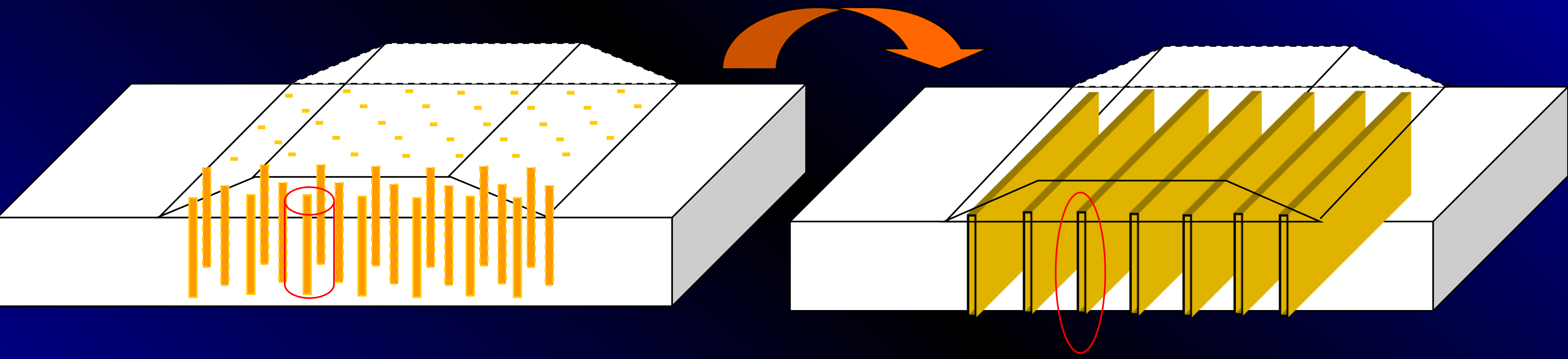

Maintain geometric equivalence

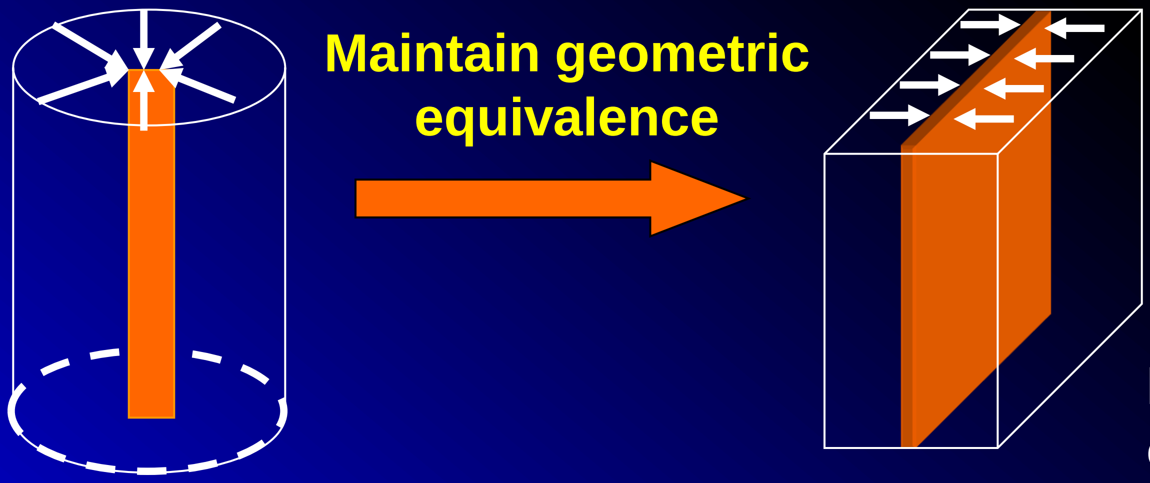

Reduce the convergence time and require less computer memory

Must give the same consolidation response

Conversion of an Axisymmetric Unit Cell into Plane Strain

Indraratna et al., 2000 & 2005

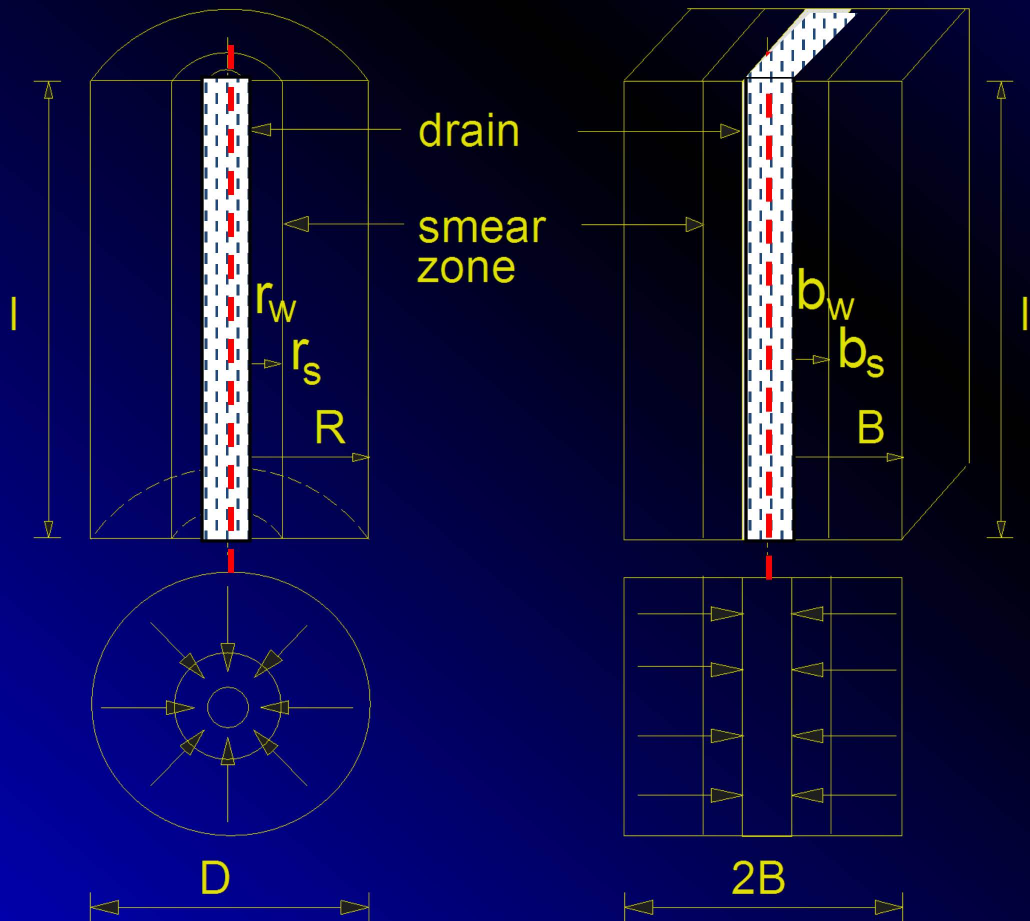

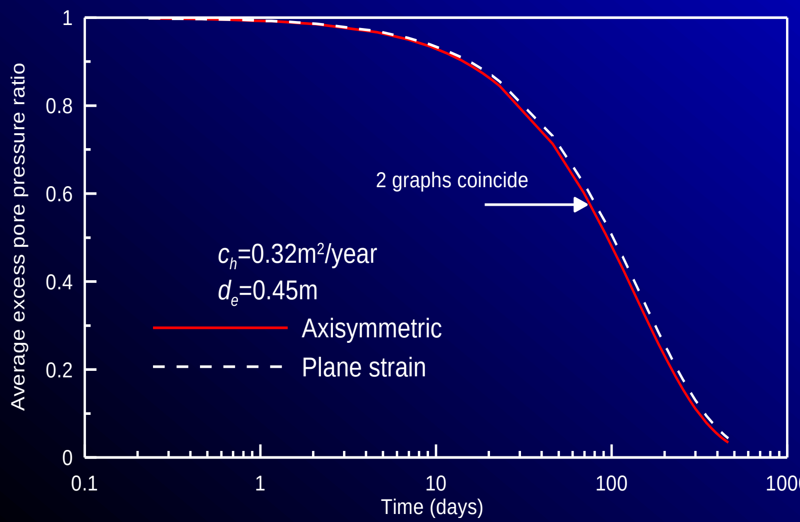

Conversion must give the **SAME** time-settlement curve

$$k_{hp} = \frac{k_h \left[\alpha + (\beta) \frac{k_{hp}}{k'_{hp}} + \frac{4l^2}{3B} \frac{k_{hp}}{q_{wp}} \right]}{\left[\ln\left(\frac{n}{s}\right) + \left(\frac{k_h}{k'_h}\right) \ln(s) - 0.75 + \frac{2\pi l^2}{3} \frac{k_h}{q_w} \right]}$$

Normalized average excess pore pressure in axisymmetric condition with vacuum (Indraratna et al., 2005), CGJ

$$\frac{\bar{u}}{\bar{u}_o} = \left(1 + \frac{\bar{u}_{vac}}{\bar{u}_o}\right) exp\left(-\frac{8T_h}{\mu}\right) - \frac{\bar{u}_{vac}}{\bar{u}_0}$$

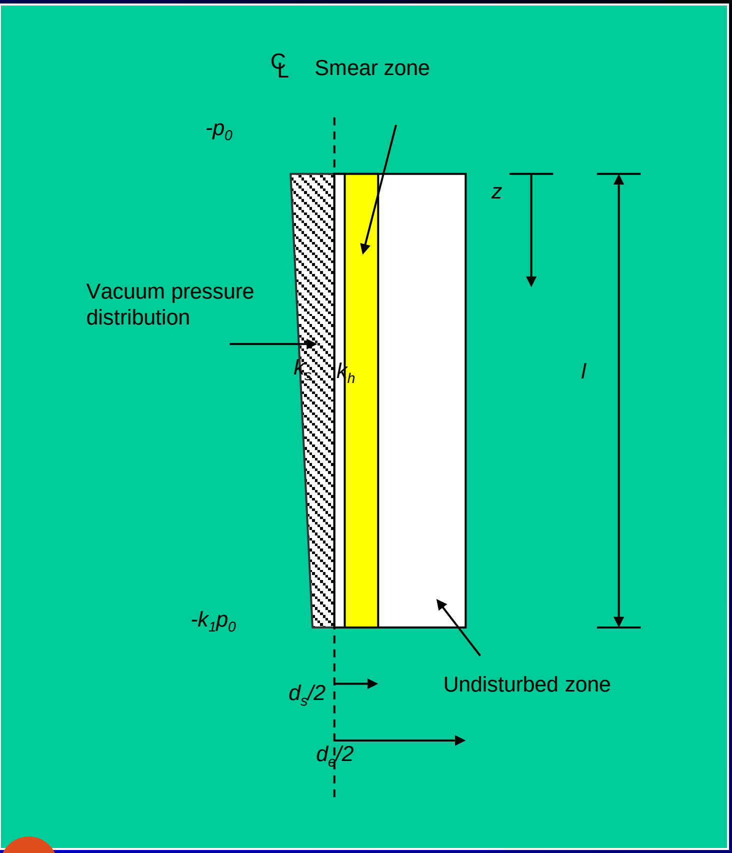

$\bar{u}_0$ = initial pore pressure

$\bar{u}$ = pore pressure at time t (average values)

T_h = time factor

$\bar{u}_{vac}$ = average applied vacuum pressure

$$\mu = \ln\left(\frac{n}{s}\right) + \left(\frac{k_h}{k'_h}\right)\ln(s) - 0.75 + \frac{2\pi l^2}{3}\frac{k_h}{q_w}$$

k_h = undisturbed horizontal permeability

k'_h = smear zone permeability

Applications at Port of Brisbane

Tough Luck! No Vertical Drains here

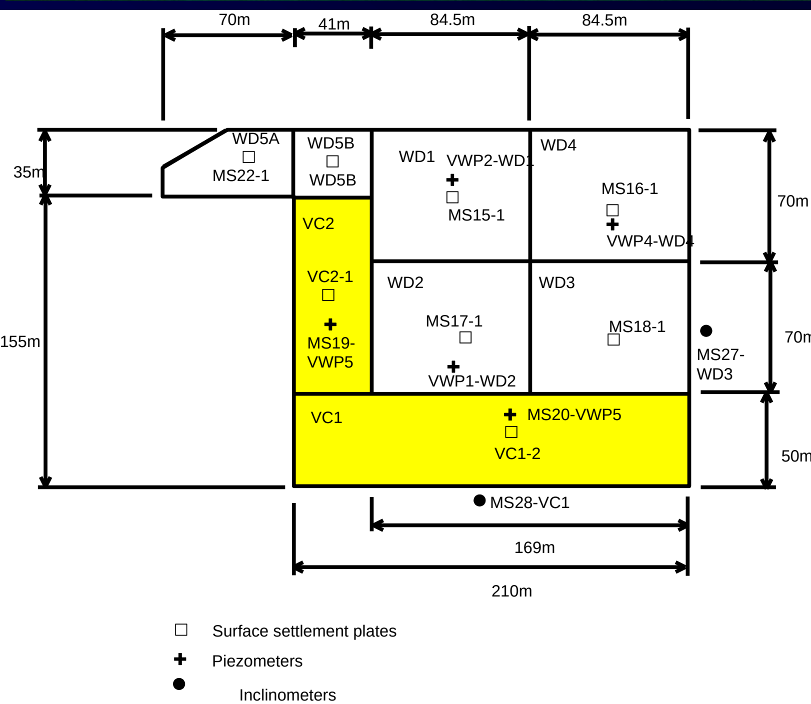

Plan view

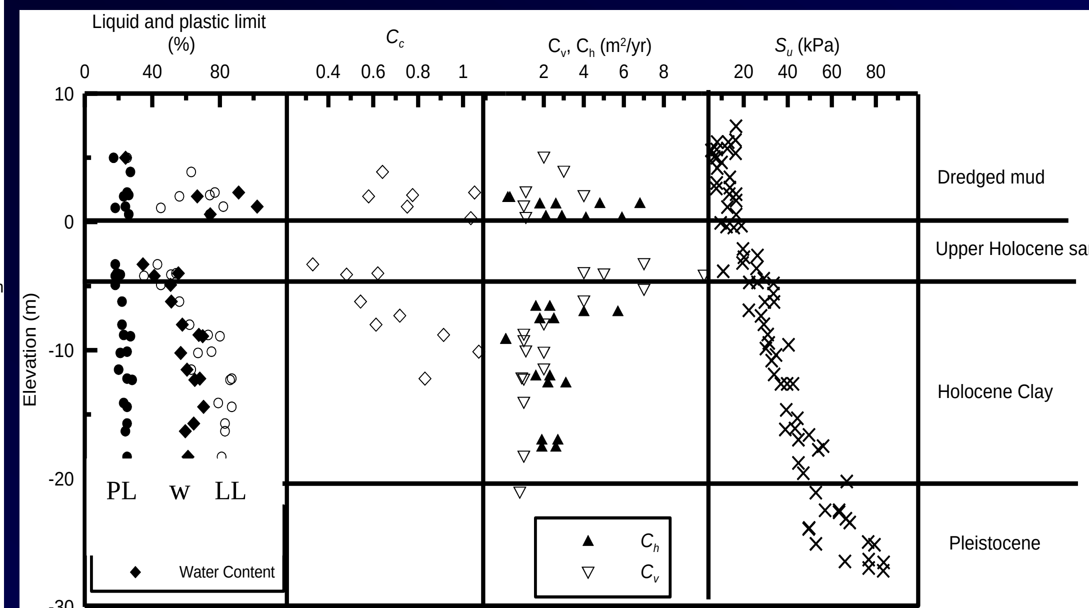

Soil Properties

3D modelling at corner of embankment or at marine boundary

Effect of vacuum application (negative movements) may extend more than 10 m from the edge of the embankment

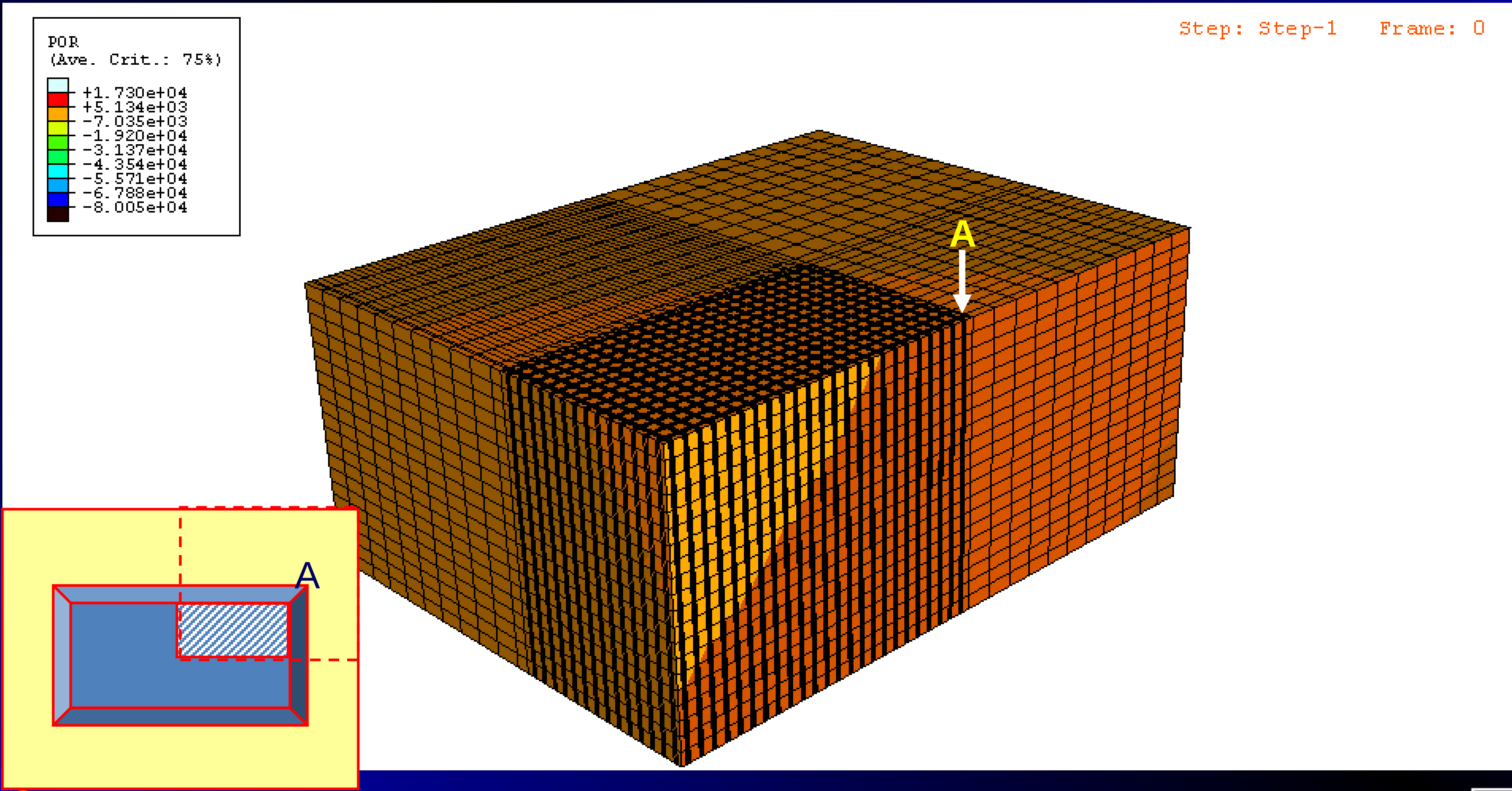

Time-Settlement, Pore Pressure & Lateral Yielding Response

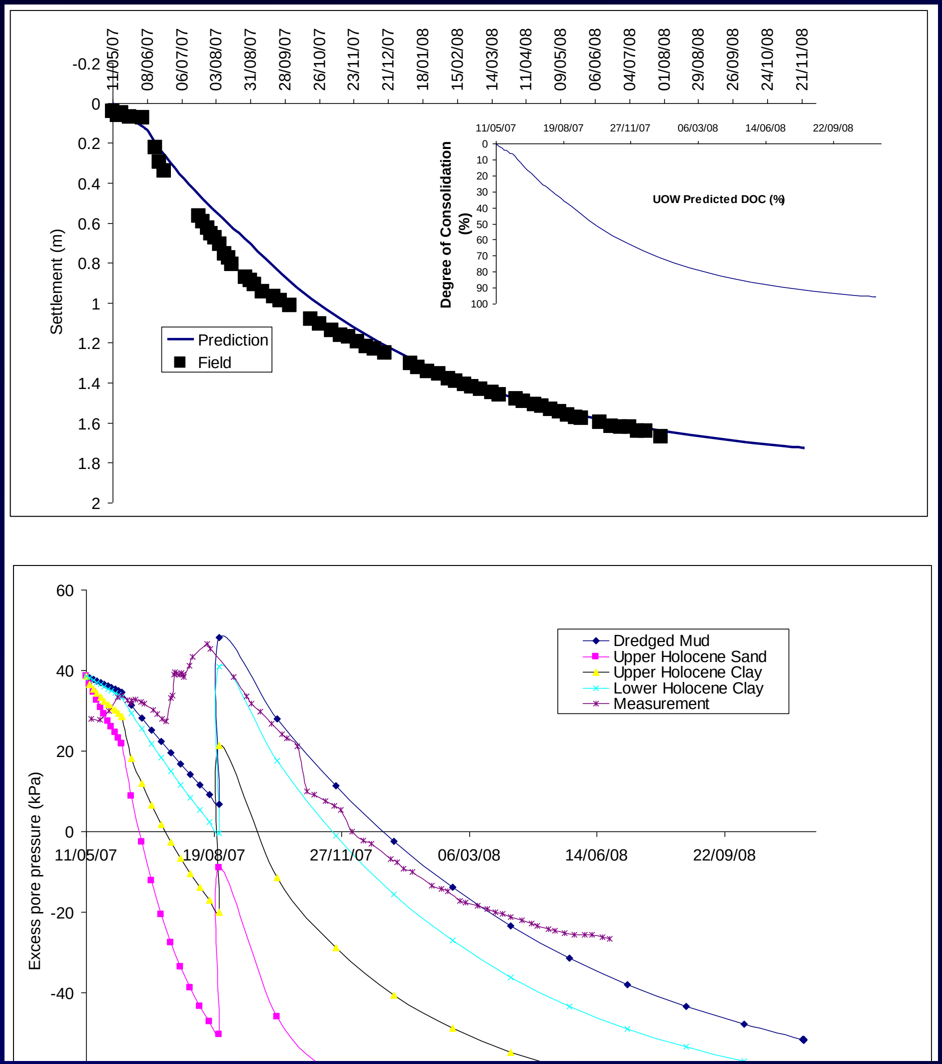

(a) Settlement and (b) excess pore pressure for a typical vacuum site

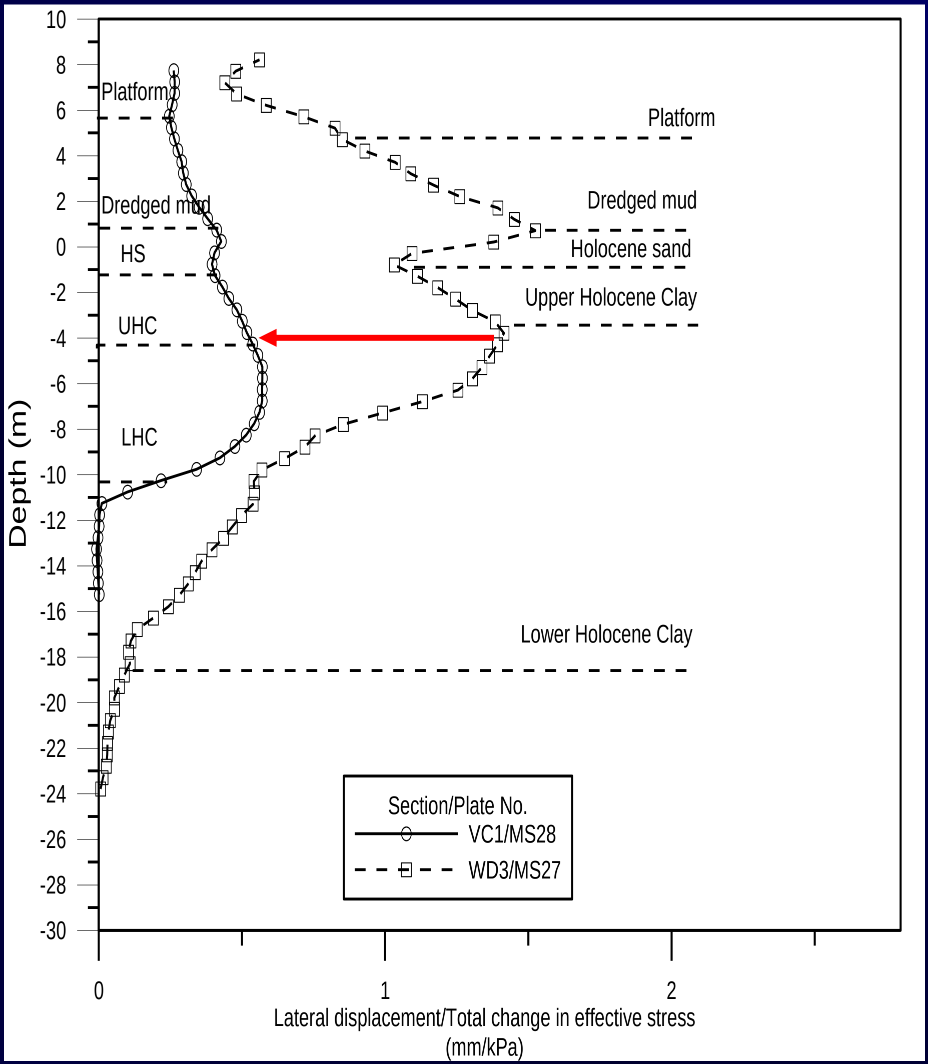

(b) Reduction of lateral displacement for a typical vacuum site

Part A + Part B: PVD Applications to Rail Embankment at Sandgate and FEM Analysis

Class A Prediction (Indraratna et al. 2010; ASCE, JGGE, Vol. 136(5), 686-696)

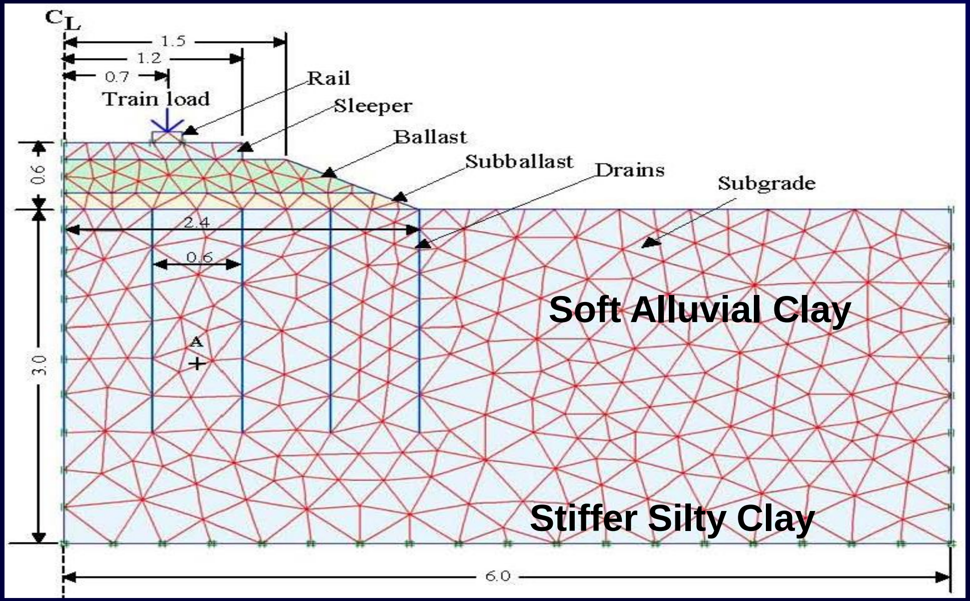

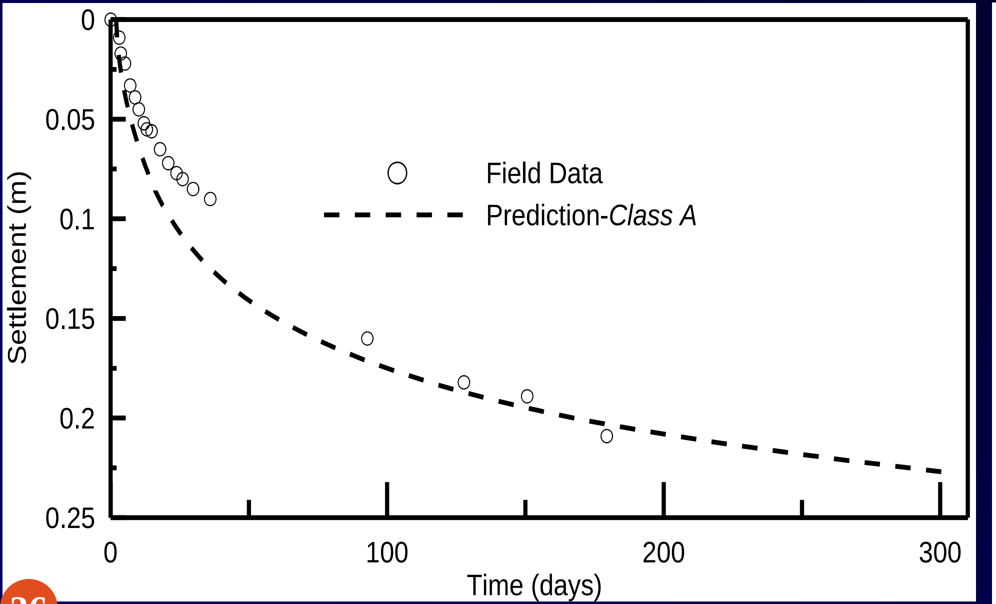

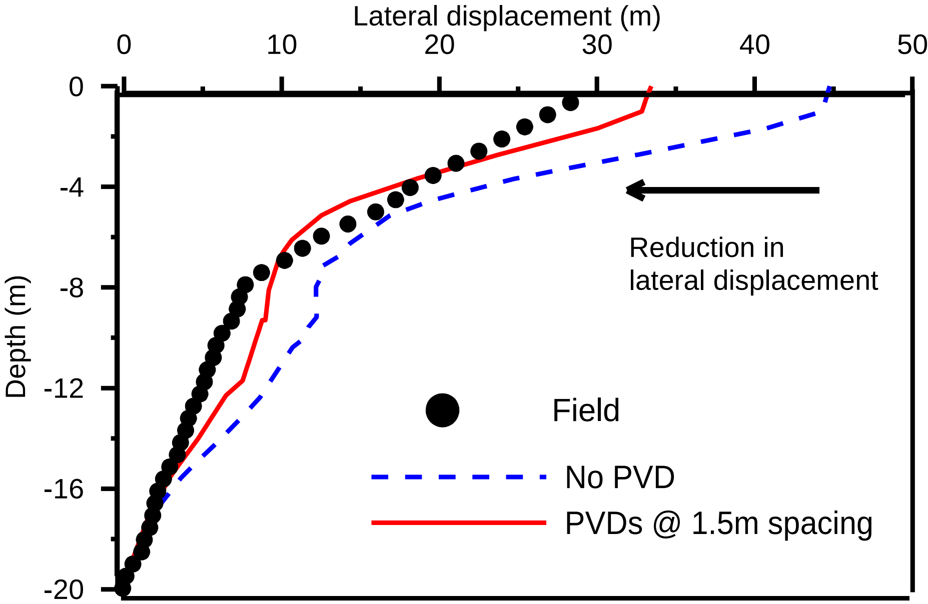

Conclusions

- Geogrids increase confining pressure and reduce particle dilation and breakage in rail tracks.
- Vacuum preloading effectively controls excess pore pressure and lateral displacement of soft soil. VP is often the ideal choice, where lateral movement at a marine boundary needs to be curbed.
- PVDs effectively mitigate the build-up of excess PWP under high cyclic loading (e.g. applications to railways and airport runways).
- DEM models are most useful to analyse track degradation, compared to current empirical assessments.
- Fully-instrumented Field trials are imperative to study complex issues of track behaviour and for performance verification.

Acknowledgment

- Australian Research Council (ARC) for substantial funding
- Past and Present research students, Research Associates and Technical Staff
- Industry Organisations: RailCorp (NSW), ARTC, QLD Rail, ARUP, Coffey Geotechnics, Douglas Partners. Roads & Traffic Authority, Queensland Department of Main Roads, Port of Brisbane Corporation

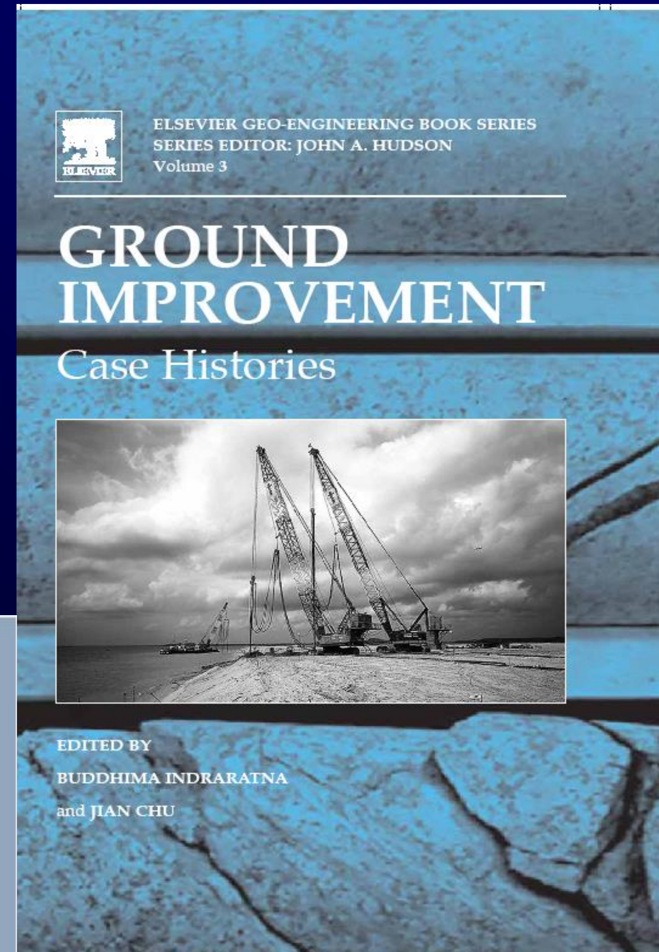

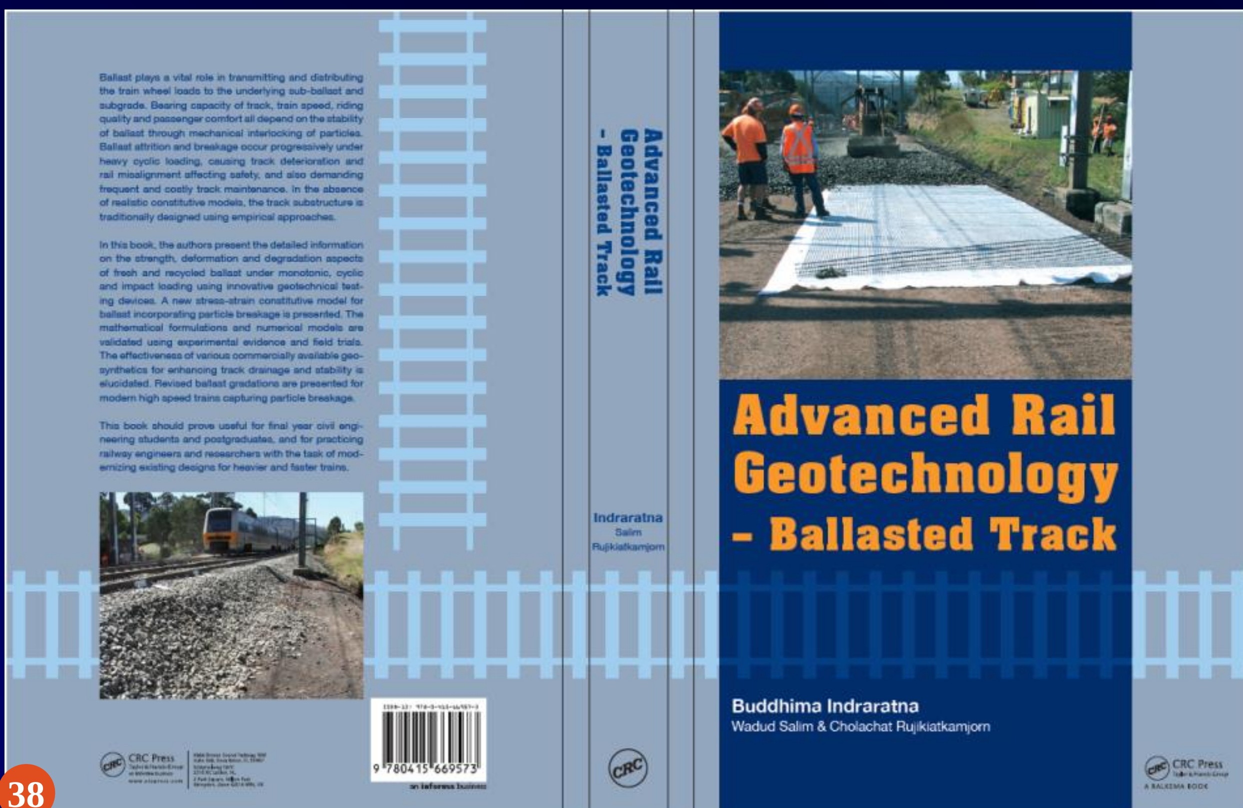

Thank You!